Multiple UAVs as Relays: Multi-hop Single Link versus Multiple Dual-hop Links

Yunfei Chen, *Senior Member, IEEE,* Nan Zhao, *Senior Member, IEEE*, Zhiguo Ding, *Senior Member, IEEE,* Mohamed-Slim Alouini, *Fellow, IEEE*

Abstract

Unmanned aerial vehicles (UAVs) have found many important applications in communications. They can serve as either aerial base stations or mobile relays to improve the quality of services. In this paper, we study the use of multiple UAVs in relaying. Considering two typical uses of multiple UAVs as relays that form either a single multi-hop link or multiple dual-hop links, we first optimize the placement of the UAVs by maximizing the end-to-end signal-to-noise ratio for three useful channel models and two common relaying protocols. Based on the optimum placement, the two relaying setups are then compared in terms of outage and bit error rate. Numerical results show that the dual-hop multi-link option is better than the multi-hop single link option when the air-to-ground path loss parameters depend on the UAV positions. Otherwise, the dual-hop option is only better when the source-to-destination distance is small. Also, decode-and-forward UAVs provide better performances than amplify-and-forward UAVs. The investigation also reveals the effects of important system parameters on the optimum UAV positions and the relaying performances to provide useful design guidelines.

I. Introduction

Unmanned aerial vehicles (UAVs) have seen a lot of new developments in recent years, due to their decreasing cost and increasing functionality [1]. One of their important applications

Yunfei Chen is with the School of Engineering, University of Warwick, Coventry, UK, CV4 7AL. (e-mail: Yunfei.Chen@warwick.ac.uk.)

Nan Zhao is with the School of Inform. and Commun. Eng., Dalian University of Technology, Dalian, 116024, P. R. China (e-mail:zhaonan@dlut.edu.cn)

Z. Ding is with School of Electrical and Electronic Engineering, the University of Manchester, Manchester, M13 9PL, UK (email: Zhiguo.ding@manchester.ac.uk)

Mohamed-Slim Alouini is with the EE program, King Abdullah University of Science and Technology, Thuwal, Mekkah Province, Saudi Arabia (e-mail: slim.alouini@kaust.edu.sa).

is in communications systems as either an aerial base station or as a mobile relay [2]. For example, in an urban area where traffic overloading often occurs or in a rural area where fixed ground infrastructure is not cost-efficient, UAVs can be deployed as aerial base stations to provide good quality of experience or seamless coverage [3], [4]. In the aftermath of a disaster when communications infrastructure is damaged, UAVs can also be used to relay the urgent messages from the ground users in the affected area to a remote base station for life-saving search and rescue missions [5] - [7]. More UAV communications applications include device-to-device communications [8], cellular networks [9], caching [10] and data off-loading [11]. This paper focuses on the second application where UAVs are used as relays.

There have been quite a few works on the use of UAVs as relays. For instance, reference [12] studied the maximization of throughput by taking the mobility of the UAV into account. Reference [13] considered the maximization of the secrecy rate by assuming a moving UAV for relaying. In another seminal paper [14], a variable-rate relaying approach was proposed to maximize the achievable rate of the system when a fixed-wing UAV was used such that severe limitation imposed by the UAV mobility has to be accounted for. In [15], the outage performance of a UAV network was analyzed where one UAV acts as a relay between the ground station and other UAVs. In [16], the ergodic capacity was maximized with a constraint on the symbol error rate to find the best position of the UAV in a relaying system. Reference [17] considered a similar problem, but the position of the UAV was optimized for a multi-rate network. As well, in [18], the best position of the UAV was studied with respect to the flow rate for a relaying system, in [19], the best position of the relaying UAV was studied by trying to maximize the connectivity of the whole network, while in [20], the best position of the relaying UAV was discussed for a system where the relaying UAV serves an aerial base station that covers several ground users instead of serving the ground users directly.

All of the above works have provided very useful insights on the designs of UAV relaying schemes. However, most of these works only considered the use of a single UAV as a relay, and none of them has considered the employment of multiple UAVs as relays. Owing to the fast development of electronics and mechanics, UAVs are becoming cheaper and more powerful. Consequently, many civil and military applications are proposing the use of multiple UAVs as a swarm or a flock for greater benefits [21], [22]. Hence, there is significant interest in the design of a UAV relaying system when multiple UAVs are used as relays. Several challenges for such a design are foreseeable. For example, the positions of these UAV relays need to be

carefully chosen for their best relaying performances. Similar problem has been studied for the conventional relaying system. To name a few, reference [23] studied the optimal relay assignment and placement to minimize the average probability of error in a sensor network. References [24] and [25] considered the optimum relay placement in a two-hop relaying system to minimize the end-to-end symbol error rate. Reference [26] derived the outage probability of a multi-hop free-space optical link with obstacles and infeasible regions and then optimized the relay positions to minimize the outage probability. Reference [27] considered the relay placement problem in wireless sensor networks with routing path selection. These works mainly assumed identical links on a 1D line or 2D surface. Also, they did not consider UAV channels. UAV relaying is more complicated in that the air-to-air link and the air-to-ground link are asymmetric and that relaying happens in a 3D space. Thus, the problem considered in this paper is different from those studied in the literature. Also, it is important to know whether one should use these UAVs to form a relaying system with a single communications link consisting of multiple hops or to form a relaying system with multiple relaying links but each link only has one UAV for dual-hop communications.

In this paper, we tackle with these challenges by studying the use of multiple UAVs in relaying. To do this, we first study the optimum positions of the UAVs in two typical relaying settings, where multiple UAVs form either a single multi-hop link or multiple dual-hop links. Analytical equations for the best altitudes and distances are derived by maximizing the end-to-end signal-to-noise ratio (SNR). In both settings, amplify-and-forward (AF) and decode-and-forward (DF) relaying protocols are considered. Using these optimum positions, the outage and the bit error rate performances of both settings are then derived and compared to determine the best way of deploying multiple UAVs. Numerical results show that the multiple dual-hop links are preferred when the parameters of the air-to-ground path loss models depend on the UAV positions. Otherwise, a multi-hop single link is preferred when the source-to-destination distance is large. They also show that DF outperforms AF for multiple UAVs. The effects of various system parameters on the optimum UAV positions and the relaying performances are also revealed to provide useful design guidelines.

The main contributions of this work can be summarized as follows:

- For the first time in the literature, it studies two different settings of multiple UAVs as either multiple hops or multiple links in UAV relaying.
- It derives the analytical equations that determine the optimum altitudes and distances of

UAV relays to maximize the approximate average end-to-end SNR for best performance.

- It analyzes the performances of different settings in terms of outage probability and bit error rate for both AF and DF protocols.
- The derivation and the comparison are conducted by using three realistic UAV channel models in a 3D space with asymmetric air-to-air and air-to-ground links.
- The effects of various important system parameters on the optimum settings are examined to provide useful design guidelines.

The rest of the paper is organized as follows. In Section II, the system model used in this paper is explained. Section III derives the optimum placement of the UAVs. Using the derived optimum placement, the performances of UAV relaying systems are analyzed in Section IV. Section V presents the numerical results. Finally, conclusions are drawn in Section VI.

II. System Model

The relaying systems considered in this paper are shown in Fig. 1. In part (a), two ground stations are used as source and destination nodes, and they are connected by $N-1$ UAVs, $N \geq 3$, where the first UAV is d_1 meters away from the source, the second UAV is d_2 meters away from the source and the last UAV is d_{N-1} meters away from the source. Thus, the distances between the UAVs is $d_n - d_{n-1}$, where $n = 2, 3, \cdots, N-1$. The distance between the two ground stations is d meters. All the UAVs have the same altitude of h meters. This gives the best performance. The reason is that, if they have different altitudes, there will be a vertical distance between two UAVs. In this case, according to the geometric theory, their distance becomes the square root of the sum of the squared vertical distance and the squared horizontal distance. This will be larger than their horizontal distance. Hence, the performance degrades due to a larger power loss. Adaptive altitudes may only be useful when the propagation environments are different for different UAVs, while this work assumes the same environment for all UAVs. In part (b), two ground stations are still connected by $N-1$ UAVs but instead of forming a multi-hop link, they form $N-1$ relaying links assisted by the $N-1$ UAVs as independent dual-hop links. Each UAV has an altitude of h_n meters from the ground and a distance of d_n meters away from the source, $n = 1, 2, \cdots, N-1$. In this case, the altitudes for different UAVs are different but their optimal altitudes will be shown later to be the same, as this is determined by the propagation environment. The total distance between the two ground stations is still d meters. Denote h_{min} as the minimum altitude for the safe flight of the UAV, so that $h \geq h_{min}$ and $h_n \geq h_{min}$.

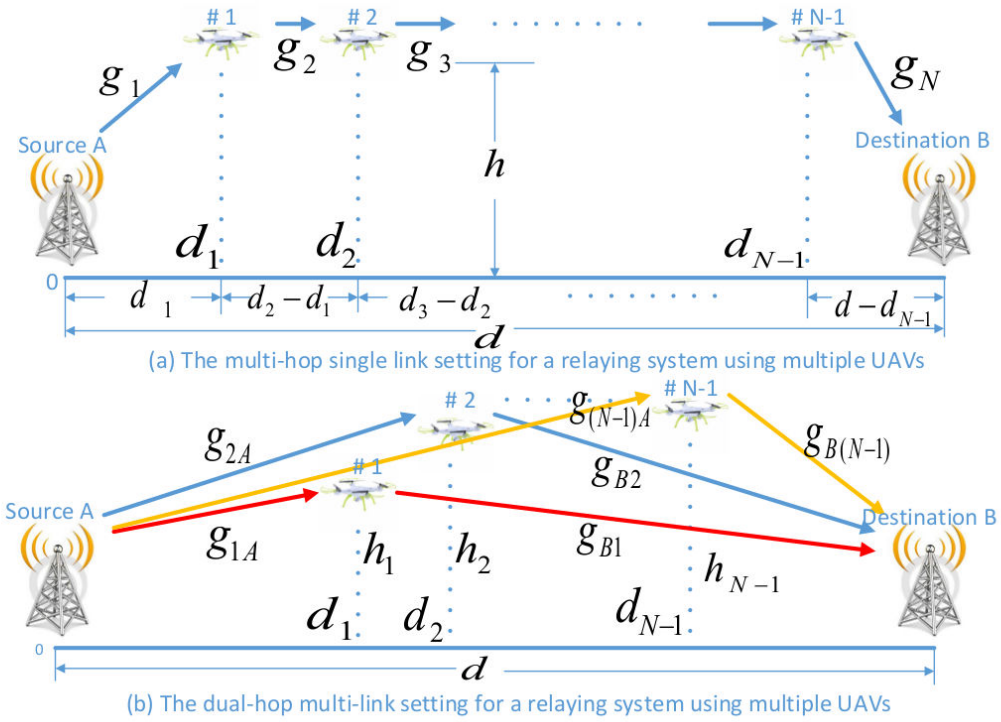

Figure 1. Diagrams for the multi-hop single link setting and the dual-hop multi-link setting of the relaying system.

All UAVs adopt orthogonal channels by transmitting signals in different time slots but at the same frequency band to avoid interference and to simplify the design. For the multi-hop setup, NT seconds will be required to complete the whole transmission, where T is the time duration of the transmission in each hop and N is the number of hops. For the dual-hop setup, the source node broadcasts the information in the first T seconds, and then each of the $N-1$ UAVs forwards the received information to the destination node in their designated time slots sequentially to avoid interference at the destination. In this case, the total time required to complete the transmission is still NT seconds. Thus, the two setups have the same total transmission time or latency. Since they transmit signals over the same frequency band, they have the same spectral efficiency as well. It is possible for different UAVs to be assigned different frequency bands to enable simultaneous operations to reduce the latency, at the cost of a reduced spectral efficiency due to increased bandwidth required.

The two settings in Fig. 1 are two typical uses of multiple relays. It is also possible to use other

settings. For example, the numbers of UAVs in each hop can be different, or different links may have different hops. They can be considered as tradeoffs between distance and reliability. These different relaying protocols offer flexibility, but they also lead to high networking overhead and complicated control and synchronization due to dissimilar link settings. For aerial communications with remotely controlled moving nodes, this may not be preferable. Another issue related to these protocols is the topology of the UAV relaying network. A detailed investigation of different relaying protocols and their associated topologies can be an interesting future research topic but is beyond the scope of the current work.

Note that the air-to-air channels in UAV communications are normally better than the air-to-ground channels, as the path loss can be described by free-space propagation and is dominant with less fading in the air-to-air channels, while fading may be dominant in the air-to-ground channels due to objects near the ground stations, in addition to more severe path loss [28]. Nevertheless, all channels are assumed to have both path loss and fading. This leads to the following observations. For the multi-hop single link setting, the communications distances are shorter and most communications happen in the better air-to-air channels between different UAVs with less power loss, but it does not have any diversity gain, as there is only a single link. On the other hand, for the dual-hop multi-link setting, the communications distances are longer and all communications happen in the worse air-to-ground channels between UAVs and ground stations, but it has diversity gain due to the multiple relaying links. The diversity gain is the rate at which the performance improves with signal-to-noise ratio, and it is proportional to the number of independent links from the source to the destination in the relaying system [29]. Thus, it is interesting to know which setting offers the best overall performance. In order to do this, the values of d_n, h_n and h need to be optimized so that one can compare the best possible performances of both settings, which will be done in the next section. Next, we will discuss the channel models.

Assume that the path loss for the air-to-air channel can be expressed as

$$L_{AA}(r) = \alpha_1 10 \log_{10} r + \eta_1, \tag{1}$$

where α_1 is the path loss exponent, r is the distance between two nodes and η_1 is the path loss at the reference point (1 meter in this case). This model applies to the channels between UAVs in both part (a) and part (b) of Fig. 1. In free-space propagation, according to the Friis

equation, one will have $\alpha_1 = 2$ and $\eta_1 = 10\log_{10}\left(\frac{4\pi f}{c}\right)^2$, where f is the carrier frequency and $c = 3 \times 10^8 m/s$ is the speed of light.

Similarly, the path loss for the air-to-ground channel can be expressed as

$$L_{AG}(r) = \alpha_2 10\log_{10} r + \eta_2, \tag{2}$$

where α_2, r and η_2 are the path loss exponent, the distance and the path loss at the reference point of the air-to-ground channel, respectively. This model applies to the channel between the source node and the first UAV or the channel between the destination node and the last UAV.

The above equations are for the dB value of the path loss. For the absolute value, the air-to-air and air-to-ground path loss models are

$$U(r) = 10^{\frac{L_{AA}(r)}{10}} = \beta_1 r^{\alpha_1}, \tag{3}$$

and

$$V(r) = 10^{\frac{L_{AG}(r)}{10}} = \beta_2 r^{\alpha_2}, \tag{4}$$

respectively, where $\beta_1 = 10^{\frac{\eta_1}{10}}$ and $\beta_2 = 10^{\frac{\eta_2}{10}}$. For free-space propagation, $\eta_1 = 10\log_{10}\left(\frac{4\pi f}{c}\right)^2$ so that $\beta_1 = \left(\frac{4\pi f}{c}\right)^2$.

A. Type A Channel Model

In this type, the path loss models have constant path loss exponent and reference path loss. It has been revealed in many works that the air-to-air channel is very close to a free-space propagation scenario. We use the results in [31] so that Type A channel model is given by

$$\begin{aligned} \alpha_1 &= 2.05, \\ \alpha_2 &= 2.32, \\ \beta_1 &= \left(\frac{4\pi f}{c}\right)^2, \\ \beta_2 &= \left(\frac{4\pi f}{c}\right)^2, \end{aligned} \tag{5}$$

where the air-to-ground channel has a larger path loss exponent than the air-to-air channel does. A use case for this model is an aerial wireless sensor network, where several UAVs equipped with sensors and radio devices fly over an area of interest to sense and collect data. More details can be found in [31].

B. Type B Channel Model

In the second type, the air-to-air channel is determined by the Friis equation, while the air-to-ground channel follows the model in [32] to give

$$\begin{aligned}
&\alpha_1 = 2,\\
&\alpha_2 = 2,\\
&\beta_1 = \left(\frac{4\pi f}{c}\right)^2,\\
&\beta_2 = 10^{\frac{B}{10}+\frac{A}{10+10a'e^{-b'(\theta-a')}}},
\end{aligned} \tag{6}$$

where $A = \eta_{LOS} - \eta_{NLOS}$, $B = 10\log_{10}\left(\frac{4\pi f}{c}\right)^2 + \eta_{NLOS}$, $\theta = \frac{180}{\pi}\arctan(\frac{h}{d_1})$ is the angle of elevation, and a', b', η_{LOS} and η_{NLOS} depend on the propagation environment. For suburban areas, $a' = 5.0188$, $b' = 0.3511$, $\eta_{LOS} = 0.1dB$ and $\eta_{NLOS} = 21dB$. Note that the path loss model here is also a function of the altitude h through the angle of elevation θ in β_2 in (6). Increasing h will make the air-to-ground link closer to line of sight but at the same time increases path loss [32]. Thus, the optimum altitude may exist. A use case for this model is a terrestrial broadband radio access system, where the UAV acts as an aerial base station to provide coverage for ground users in the system [32].

C. Type C Channel Model

In the third type, the air-to-air channel is still determined by free-space propagation, while the air-to-ground channel follows the model in [33] such that

$$\begin{aligned}
&\alpha_1 = 2,\\
&\alpha_2 = 3.9 - 0.9\log_{10} h,\\
&\beta_1 = \left(\frac{4\pi f}{c}\right)^2,\\
&\beta_2 = 10^{-0.85}h^{2.05},
\end{aligned} \tag{7}$$

where h is the altitude. As reported in [33],$1 \leq h \leq 120$ meters in order for the model to be valid. In this case, both the path loss exponent and the reference path loss in the air-to-ground channel depend on the altitude but not on the distance. A use case for this model is the LTE system, where the UAV acts as an aerial base station to serve the user equipment in the network, as studied in [33].

D. End-to-End Performance

Using the above models, the end-to-end SNR of multi-hop AF relaying is shown as [30]

$$\gamma_{ee1} = \left[\prod_{i=1}^{N}(1+\frac{1}{\gamma_i}) - 1\right]^{-1}, \tag{8}$$

where γ_i is the SNR of the i-th hop with

$$\gamma_i = \frac{P_i|g_i|^2}{W_i \cdot U(r_i)}, i = 1 \; or \; N,$$
$$\gamma_i = \frac{P_i|g_i|^2}{W_i \cdot V(r_i)}, i = 2, \cdots, N-1, \tag{9}$$

P_i is the transmission power of the i-th hop so that P_1 is the transmission power of the source node, P_2 is the transmission power of UAV 1 and P_N is the transmission power of UAV $N-1$, g_i is the fading coefficient of the i-th hop following Nakagami-m fading, W_i is the noise power in the i-th hop so that W_1 is the noise power at UAV 1, W_{N-1} is the noise power at UAV $N-1$ and W_N is the noise power at the destination node, and r_i is the distance of the i-th hop so that $r_1 = \sqrt{h^2 + d_1^2}$, $r_i = d_i - d_{i-1}$ for $i = 2, \cdots, N-1$ and $r_N = \sqrt{h^2 + (d - d_{N-1})^2}$. Note that, although both small-scale fading and large-scale path loss are considered in (9), in practice, the direct use of (9) would lead to optimum positions that require knowledge of the instantaneous channel state information and hence the optimum positions of the UAVs have to be adjusted in real-time with energy-consuming acceleration and deceleration. A more practical solution is to use the average SNR to optimize the UAV positions. This will give a suboptimal or rough estimate of the optimum positions but can save energy for UAV operations.

We assume that g_i follows a Nakagami m distribution with parameter m and average fading power Ω and that all the fading coefficients are independent. Hence, we assume that both air-to-air channels and air-to-ground channels suffer from path loss and fading. The Nakagami m distribution is a very flexible fading model [35]. For example, when $m = 1$, it represents Rayleigh fading, and when $m \to \infty$, it represents a non-fading channel. It can also approximate the Rician fading with a one-to-one correspondence between m and the Rician K factor [35]. Although the Rician model is commonly used in UAV communications, it has been reported in several works that the Nakagami model can be used to describe UAV channels too [36], [37].

For multi-hop DF relaying, the end-to-end SNR can be derived as

$$\gamma_{ee2} = \min\{\gamma_1, \gamma_2, \cdots, \gamma_N\}, \tag{10}$$

where γ_i, $i = 1, 2, \cdots, N$ are defined as before.

The above is for the multi-hop setting. For the dual-hop multi-link setting, using selection combining, the overall SNR of dual-hop AF that chooses the link with the largest end-to-end link SNR is given by

$$\chi_{ee1} = \max_{n}\{\frac{\gamma_{nA}\gamma_{Bn}}{\gamma_{nA}+\gamma_{Bn}+1}\}, \tag{11}$$

where $n = 1, 2, \cdots, N-1$ is the link index, $\frac{\gamma_{nA}\gamma_{Bn}}{\gamma_{nA}+\gamma_{Bn}+1}$ is the end-to-end SNR of the n-th link used for selection, $\gamma_{nA} = \frac{P_A|g_{nA}|^2}{W_n \cdot V(r_{nA})}$, $\gamma_{Bn} = \frac{P_n|g_{Bn}|^2}{W_B \cdot V(r_{Bn})}$, P_A is the transmission power of the source node, P_n is the transmission power of the n-th UAV relay, g_{nA} is the fading coefficient of the channel between the source node and the n-th UAV relay, W_n is the noise power at the n-th UAV, $r_{nA} = \sqrt{h_n^2 + d_n^2}$ is the distance between the source node and the n-th UAV, g_{Bn} is the fading coefficient of the channel between the $n-th$ UAV relay and the destination node, W_B is the noise power at the destination, and $r_{Bn} = \sqrt{h_n^2 + (d-d_n)^2}$ is the distance between the n-th UAV and the destination. Also, g_{nA} and g_{Bn} follow Nakagami m distributions with parameter m and average fading power Ω. Thus, (11) is obtained by choosing the dual-hop link with the largest link SNR from source to destination based on selection combining.

Note that selection combining is considered in this work due to its simplicity. There are other combining schemes, such as maximum ratio combining or equal-gain combining. These schemes often have better performances than selection combining but they require more channel knowledge as well as incur more network overheads, which may not be desirable in the considered applications, especially in relaying systems with more than one hop and more than two nodes. Thus, they are not investigated here.

For multiple links using dual-hop DF, the end-to-end SNR is given by

$$\chi_{ee2} = \max_{n}\{\min\{\gamma_{nA}, \gamma_{Bn}\}\}. \tag{12}$$

We will maximize the end-to-end SNR for different relaying protocols with respect to the values of d_n, h_n and h in the next section.

III. Placement Optimization

In order to compare the multi-hop single link setting with the dual-hop multi-link setting, we need to find the optimum altitudes and distances that maximize the end-to-end SNR. We will do this for three different types of channel models. Note that these models are suitable for different applications in different scenarios such that there is no performance comparison between them.

A. Type A Channel Model

We start with the exact end-to-end SNR for multi-hop AF, γ_{ee1}, as given in (8). From (8), maximizing γ_{ee1} is equivalent to minimizing $\prod_{i=1}^{N}(1+\frac{1}{\gamma_i})$. Thus, using (9), we need to minimize the following value

$$H_{ee1}(h, d_1, \cdots, d_{N-1}) = \left(1 + \frac{W_1\beta_2(h^2 + d_1^2)^{\frac{\alpha_2}{2}}}{P_1|g_1|^2}\right) \left(1 + \frac{W_N\beta_2(h^2 + (d - d_{N-1})^2)^{\frac{\alpha_2}{2}}}{P_N|g_N|^2}\right) \prod_{i=2}^{N-1}\left(1 + \frac{W_i\beta_1(d_i - d_{i-1})^{\alpha_1}}{P_i|g_i|^2}\right), h \geq h_{min}, \quad (13)$$

with respect to the altitude and the relevant distances. However, this optimization would give optimum altitudes and distances as functions of the fading coefficients $g_1, g_2, \cdots, g_N$. Since these fading coefficients are random, or at least change from time to time, the optimum altitudes and distances have to change from time to time too. This may not be desirable in practice, as acceleration and deceleration of the UAVs will consume a significant amount of energy. Also, it may be difficult to obtain the channel state information. A simpler alternative is to first take the average of (13) over the fading coefficients to eliminate the fading coefficients and then optimize the average. Since the fading coefficients follow independent and identical Nakagami m distributions with parameter m and average fading power Ω, the average of (13) can be calculated as

$$J_{ee1}(h, d_1, \cdots, d_{N-1}) = \left(1 + \frac{W_1\beta_2(h^2 + d_1^2)^{\frac{\alpha_2}{2}}}{P_1\Omega}\right) \left(1 + \frac{W_N\beta_2(h^2 + (d - d_{N-1})^2)^{\frac{\alpha_2}{2}}}{P_N\Omega}\right) \prod_{i=2}^{N-1}\left(1 + \frac{W_i\beta_1(d_i - d_{i-1})^{\alpha_1}}{P_i\Omega}\right), h \geq h_{min}, \quad (14)$$

where several integrals of $\int_0^\infty(1 + \frac{c}{x})(\frac{m}{\Omega})^m\frac{x^{m-1}}{\Gamma(m)}e^{-\frac{m}{\Omega}x}dx$ are solved using [34, eq. (3.381.4)] to give $(1 + \frac{c}{\Omega})$, c is a constant that equals to different values for different terms in (13) and $(\frac{m}{\Omega})^m\frac{x^{m-1}}{\Gamma(m)}e^{-\frac{m}{\Omega}x}$ is the probability density function of $|g_i|^2$ for $i = 1, 2, \cdots, N$. Hence, (14) can simply be obtained from (13) by replacing the instantaneous fading power $|g_i|^2$ with the average fading power Ω. Note that (14) is the average of (13), not the average end-to-end SNR. The average end-to-end SNR is calculated by averaging (8) over the fading coefficients. However, this calculation does not lead to any tractable expression for optimization, due to the inverse function. Thus, it is not discussed here.

We use (14) as the target function for optimization in the following. For other channel models and other SNR expressions, this method is also used. Since the fading coefficients are eliminated

by the averaging operation, the transmitters do not need the channel state information and will not have this knowledge.

It can be shown that (14) is a convex function, as its second-order derivatives with respect to h, $d_1, \cdots, d_{N-1}$ are larger than 0. Similar arguments can also be made for other objective functions, which are omitted in the paper. To optimize it by taking the first-order derivative of (14) with respect to h, one has

$$\frac{\partial J_{ee1}}{\partial h} = \left[\frac{\frac{W_1\beta_2(h^2+d_1^2)^{\frac{\alpha_2}{2}-1}\alpha_2 h}{P_1\Omega}}{1+\frac{W_1\beta_2(h^2+d_1^2)^{\frac{\alpha_2}{2}}}{P_1\Omega}} + \frac{\frac{W_N\beta_2(h^2+(d-d_{N-1})^2)^{\frac{\alpha_2}{2}-1}\alpha_2 h}{P_N\Omega}}{1+\frac{W_N\beta_2(h^2+(d-d_{N-1})^2)^{\frac{\alpha_2}{2}}}{P_N\Omega}} \right] J_{ee1}. \tag{15}$$

One can see that (15) only equals to 0 when $h = 0$. Thus, in this case, the optimum altitude would be $\hat{h} = 0$. In practice, since $h \geq h_{min}$ for safety reason, $\hat{h} = h_{min}$.

Also, by taking the first-order derivatives of (14) with respect to $d_1, d_2, \cdots, d_{N-1}$ and setting them to zero, the optimum distances, $\hat{d}_1, \hat{d}_2, \cdots, \hat{d}_{N-1}$, satisfy

$$\frac{\frac{W_1\beta_2(\hat{h}^2+\hat{d}_1^2)^{\frac{\alpha_2}{2}-1}\alpha_2\hat{d}_1}{P_1\Omega}}{1+\frac{W_1\beta_2(\hat{h}^2+\hat{d}_1^2)^{\frac{\alpha_2}{2}}}{P_1\Omega}} = \frac{\frac{W_2\beta_1\alpha_1(\hat{d}_2-\hat{d}_1)^{\alpha_1-1}}{P_2\Omega}}{1+\frac{W_2\beta_1(\hat{d}_2-\hat{d}_1)^{\alpha_1}}{P_2\Omega}} = \cdots = \frac{\frac{W_N\beta_2(\hat{h}^2+(d-\hat{d}_{N-1})^2)^{\frac{\alpha_2}{2}-1}\alpha_2(d-\hat{d}_{N-1})}{P_N\Omega}}{1+\frac{W_N\beta_2(\hat{h}^2+(d-\hat{d}_{N-1})^2)^{\frac{\alpha_2}{2}}}{P_N\Omega}}. \tag{16}$$

A special case occurs when the transmission SNRs at different nodes are the same. In this case, $\frac{P_i}{W_i} = \frac{P}{W}$ for $i = 1, 2, \cdots, N$. Thus, from (16),

$$\begin{aligned} &\hat{d}_1 = d - \hat{d}_{N-1} = \hat{b}, \\ &\hat{d}_2 - \hat{d}_1 = \hat{d}_3 - \hat{d}_2 = \cdots = \hat{d}_{N-1} - \hat{d}_{N-2} = \hat{a} = \frac{d-2\hat{b}}{N-2}, \end{aligned} \tag{17}$$

where $\hat{b}$ is determined by

$$\frac{\beta_2(\hat{h}^2+\hat{b}^2)^{\frac{\alpha_2}{2}-1}\alpha_2\hat{b}}{\frac{P\Omega}{W}+\beta_2(\hat{h}^2+\hat{b}^2)^{\frac{\alpha_2}{2}}} = \frac{\beta_1\alpha_1(\frac{d-2\hat{b}}{N-2})^{\alpha_1-1}}{\frac{P\Omega}{W}+\beta_1(\frac{d-2\hat{b}}{N-2})^{\alpha_1}}, \tag{18}$$

for $0 < \hat{b} < \frac{d}{2}$. One sees from (18) that, when the average SNR is large, the two denominators are the same and can be cancelled out at both sides of the equation. In this case, the optimum distances do not depend on the average SNR but only on the path loss model parameters, the optimum altitude and the number of hops.

Next, we focus on the multi-hop DF γ_{ee2}. Following exactly the same procedure, the objective function to be minimized in this case is

$$\begin{aligned} J_{ee2}(h, d_1, \cdots, d_{N-1}) \;=\; &\max\{\frac{W_1\beta_2(h^2+d_1^2)^{\frac{\alpha_2}{2}}}{P_1\Omega}, \frac{W_2\beta_1(d_2-d_1)^{\alpha_1}}{P_2\Omega}, \\ &\cdots, \frac{W_N\beta_2(h^2+(d-d_{N-1})^2)^{\frac{\alpha_2}{2}}}{P_N\Omega}\}, h \geq h_{min}. \end{aligned} \tag{19}$$

Each element inside the maximum function is convex, as their second-order derivatives with respect to h, $d_1, \cdots, d_{N-1}$ are larger than 0. According to the convex optimization theory [38], element-wise maximum preserves convexity so that the whole function in (19) is also convex. Similar arguments can also be made for other objective functions, which are omitted in the paper.

The optimum altitude is again $\hat{h} = h_{min}$ in practice. The optimum distances are derived from

$$\frac{W_1\beta_2(\hat{h}^2+\hat{d}_1^2)^{\frac{\alpha_2}{2}}}{P_1\Omega} = \frac{W_2\beta_1(\hat{d}_2-\hat{d}_1)^{\alpha_1}}{P_2\Omega} = \cdots = \frac{W_N\beta_2(\hat{h}^2+(d-\hat{d}_{N-1})^2)^{\frac{\alpha_2}{2}}}{P_N\Omega}. \tag{20}$$

In the special case when $\frac{P_i}{W_i} = \frac{P}{W}$, the optimum distances can be calculated from (17), where $\hat{b}$ is determined by

$$\beta_2(\hat{h}^2+\hat{b}^2)^{\frac{\alpha_2}{2}} = \beta_1(\frac{d-2\hat{b}}{N-2})^{\alpha_1}. \tag{21}$$

Next, we consider the dual-hop multi-link setting. In this case, the UAVs are independent so that h_n and d_n can be optimized separately for different links. Thus, we can optimize the link end-to-end SNR instead.

For χ_{ee1}, it can be shown that one needs to minimize the objective function

$$K_{ee1}(h_n, d_n) = \left(1+\frac{W_n\beta_2(h_n^2+d_n^2)^{\frac{\alpha_2}{2}}}{P_A\Omega}\right)(1+\frac{W_B\beta_2(h_n^2+(d-d_n)^2)^{\frac{\alpha_2}{2}}}{P_n\Omega}), h_n \geq h_{min}, \tag{22}$$

for $n = 1, 2, \cdots, N-1$. By taking the first-order derivatives of (22) with respect to h_n and d_n, it can be shown that the optimum altitude would be $\hat{h}_n = 0$ but is $\hat{h}_n = h_{min}$ in practice, and the optimum distance is derived from

$$\frac{\frac{W_n\beta_2(\hat{h}_n^2+\hat{d}_n^2)^{\frac{\alpha_2}{2}-1}\alpha_2\hat{d}_n}{P_A\Omega}}{1+\frac{W_n\beta_2(\hat{h}_n^2+\hat{d}_n^2)^{\frac{\alpha_2}{2}}}{P_A\Omega}} = \frac{\frac{W_B\beta_2(\hat{h}_n^2+(d-\hat{d}_n)^2)^{\frac{\alpha_2}{2}-1}\alpha_2(d-\hat{d}_n)}{P_n\Omega}}{1+\frac{W_B\beta_2(\hat{h}_n^2+(d-\hat{d}_n)^2)^{\frac{\alpha_2}{2}}}{P_n\Omega}}. \tag{23}$$

In the case when $\frac{P_A}{W_n} = \frac{P_n}{W_B} = \frac{P}{W}$, it can be easily derived that the optimum distance is $\hat{d}_n = \frac{d}{2}$.

For χ_{ee2}, the practical optimum altitude is $\hat{h}_n = h_{min}$ and the optimum distance is determined by

$$\frac{W_n\beta_2(\hat{h}_n^2+\hat{d}_n^2)^{\frac{\alpha_2}{2}}}{P_A\Omega} = \frac{W_B\beta_2(\hat{h}_n^2+(d-\hat{d}_n)^2)^{\frac{\alpha_2}{2}}}{P_n\Omega}. \tag{24}$$

When $\frac{P_A}{W_n} = \frac{P_n}{W_B} = \frac{P}{W}$, the optimum distance is $\hat{d}_n = \frac{d}{2}$.

In summary, for the multi-hop single link setting, the practical optimum altitude is always h_{min}, and the optimum distances can be obtained by solving $N-1$ nonlinear equations. When $\frac{P_i}{W_i} = \frac{P}{W}$, only one nonlinear equation needs to be solved. For the dual-hop multi-link setting, the practical optimum altitude is always h_{min}. The optimum distance can be found by solving one nonlinear equation. In the case of $\frac{P_A}{W_n} = \frac{P_n}{W_B}$, the optimum distance is always $\frac{d}{2}$.

B. Type B Channel Model

We start with the maximization of the exact end-to-end SNR for multi-hop AF as γ_{ee1}. The objective function is similar to that in (14), except that β_2 is replaced by $\beta_2(h,d)$ to show its dependence on h and d explicitly. The optimization method is also similar. Thus we only show the final results to reduce the redundancy in the derivation. It can be shown that the optimum altitude and distances satisfy

$$\frac{\frac{W_1}{P_1\Omega}(\hat{h}^2+\hat{d}_1^2)^{\frac{\alpha_2}{2}}[\frac{\partial\beta_2(\hat{h},\hat{d}_1)}{\partial\hat{h}}+\beta_2(\hat{h},\hat{d}_1)\frac{\alpha_2\hat{h}}{\hat{h}^2+\hat{d}_1^2}]}{1+\frac{W_1\beta_2(\hat{h},\hat{d}_1)(\hat{h}^2+\hat{d}_1^2)^{\frac{\alpha_2}{2}}}{P_1\Omega}} + \frac{\frac{W_N}{P_N\Omega}(\hat{h}^2+(d-\hat{d}_{N-1})^2)^{\frac{\alpha_2}{2}}[\frac{\partial\beta_2(\hat{h},d-\hat{d}_{N-1})}{\partial\hat{h}}+\beta_2(\hat{h},d-\hat{d}_{N-1})\frac{\alpha_2\hat{h}}{\hat{h}^2+(d-\hat{d}_{N-1})^2}]}{1+\frac{W_N\beta_2(\hat{h},d-\hat{d}_{N-1})(\hat{h}^2+(d-\hat{d}_{N-1})^2)^{\frac{\alpha_2}{2}}}{P_N\Omega}}=0, \quad (25)$$

and

$$\begin{aligned}&\frac{\frac{W_1}{P_1\Omega}(\hat{h}^2+\hat{d}_1^2)^{\frac{\alpha_2}{2}}[\frac{\partial\beta_2(\hat{h},\hat{d}_1)}{\partial\hat{d}_1}+\beta_2(\hat{h},\hat{d}_1)\frac{\alpha_2\hat{d}_1}{\hat{h}^2+\hat{d}_1^2}]}{1+\frac{W_1\beta_2(\hat{h},\hat{d}_1)(\hat{h}^2+\hat{d}_1^2)^{\frac{\alpha_2}{2}}}{P_1\Omega}}=\frac{\frac{W_2\beta_1\alpha_1(\hat{d}_2-\hat{d}_1)^{\alpha_1-1}}{P_2\Omega}}{1+\frac{W_2\beta_1(\hat{d}_2-\hat{d}_1)^{\alpha_1}}{P_2\Omega}}=\cdots\\ &=\frac{\frac{W_N}{P_N\Omega}(\hat{h}^2+(d-\hat{d}_{N-1})^2)^{\frac{\alpha_2}{2}}[\frac{\partial\beta_2(\hat{h},d-\hat{d}_{N-1})}{\partial(d-\hat{d}_{N-1})}+\beta_2(\hat{h},d-\hat{d}_{N-1})\frac{\alpha_2(d-\hat{d}_{N-1})}{\hat{h}^2+(d-\hat{d}_{N-1})^2}]}{1+\frac{W_N\beta_2(\hat{h},d-\hat{d}_{N-1})(\hat{h}^2+(d-\hat{d}_{N-1})^2)^{\frac{\alpha_2}{2}}}{P_N\Omega}},\end{aligned} \quad (26)$$

where one has from (6)

$$\begin{aligned}\frac{\partial\beta_2(h,x)}{\partial h}&=\beta_2(h,x)\frac{180xA\ln(10)}{10\pi(h^2+x^2)}\frac{a'b'e^{-b'(\frac{180}{\pi}\arctan(h/x)-a')}}{(1+a'e^{-b'(\frac{180}{\pi}\arctan(h/x)-a')})^2},\\ \frac{\partial\beta_2(h,x)}{\partial x}&=-\beta_2(h,x)\frac{180hA\ln(10)}{10\pi(h^2+x^2)}\frac{a'b'e^{-b'(\frac{180}{\pi}\arctan(h/x)-a')}}{(1+a'e^{-b'(\frac{180}{\pi}\arctan(h/x)-a')})^2}.\end{aligned} \quad (27)$$

For multi-hop DF γ_{ee2}, similarly, the optimum altitude and the optimum distances satisfy

$$\frac{\partial\beta_2(\hat{h},\hat{d}_1)}{\partial\hat{h}}+\beta_2(\hat{h},\hat{d}_1)\frac{\alpha_2\hat{h}}{\hat{h}^2+\hat{d}_1^2}=0, \quad (28)$$

and

$$\begin{aligned}&\frac{W_1}{P_1\Omega}\beta_2(\hat{h},\hat{d}_1)(\hat{h}^2+\hat{d}_1^2)^{\frac{\alpha_2}{2}}=\frac{W_2\beta_1(\hat{d}_2-\hat{d}_1)^{\alpha_1}}{P_2\Omega}=\cdots\\ &=\frac{W_N}{P_N\Omega}\beta_2(\hat{h},d-\hat{d}_{N-1})(\hat{h}^2+(d-\hat{d}_{N-1})^2)^{\frac{\alpha_2}{2}}.\end{aligned} \quad (29)$$

In the dual-hop multi-link setting, the procedures are very similar to before. In this case, for dual-hop multi-link AF χ_{ee1}, the optimum values of $\hat{h}_n$ and $\hat{d}_n$ can be solved from the following two nonlinear equations

$$\begin{aligned}
&\frac{\frac{W_n[\frac{\partial\beta_2(\hat{h}_n,\hat{d}_n)}{\partial\hat{h}_n}+\beta_2(\hat{h}_n,\hat{d}_n)\frac{\alpha_2\hat{h}_n}{\hat{h}_n^2+\hat{d}_n^2}]}{P_A\Omega(\hat{h}_n^2+\hat{d}_n^2)^{-\frac{\alpha_2}{2}}}}{1+\frac{W_n\beta_2(\hat{h}_n,\hat{d}_n)}{P_A\Omega}(\hat{h}_n^2+\hat{d}_n^2)^{\frac{\alpha_2}{2}}}+\frac{\frac{W_B[\frac{\partial\beta_2(\hat{h}_n,d-\hat{d}_n)}{\partial\hat{h}_n}+\beta_2(\hat{h}_n,d-\hat{d}_n)\frac{\alpha_2\hat{h}_n}{\hat{h}_n^2+(d-\hat{d}_n)^2}]}{P_A\Omega(\hat{h}_n^2+(d-\hat{d}_n)^2)^{-\frac{\alpha_2}{2}}}}{1+\frac{W_B\beta_2(\hat{h}_n,d-\hat{d}_n)}{P_A\Omega}(\hat{h}_n^2+(d-\hat{d}_n)^2)^{\frac{\alpha_2}{2}}}=0,\\
&\frac{\frac{W_n[\frac{\partial\beta_2(\hat{h}_n,\hat{d}_n)}{\partial\hat{d}_n}+\beta_2(\hat{h}_n,\hat{d}_n)\frac{\alpha_2\hat{d}_n}{\hat{h}_n^2+\hat{d}_n^2}]}{P_A\Omega(\hat{h}_n^2+\hat{d}_n^2)^{-\frac{\alpha_2}{2}}}}{1+\frac{W_n\beta_2(\hat{h}_n,\hat{d}_n)}{P_A\Omega}(\hat{h}_n^2+\hat{d}_n^2)^{\frac{\alpha_2}{2}}}=\frac{\frac{W_B[\frac{\partial\beta_2(\hat{h}_n,d-\hat{d}_n)}{\partial(d-\hat{d}_n)}+\beta_2(\hat{h}_n,d-\hat{d}_n)\frac{\alpha_2(d-\hat{d}_n)}{\hat{h}_n^2+(d-\hat{d}_n)^2}]}{P_A\Omega(\hat{h}_n^2+(d-\hat{d}_n)^2)^{-\frac{\alpha_2}{2}}}}{1+\frac{W_B\beta_2(\hat{h}_n,d-\hat{d}_n)}{P_A\Omega}(\hat{h}_n^2+(d-\hat{d}_n)^2)^{\frac{\alpha_2}{2}}}.
\end{aligned}\tag{30}$$

For χ_{ee2}, the two equations are

$$\begin{aligned}
&\frac{\partial\beta_2(\hat{h}_n,\hat{d}_n)}{\partial\hat{h}_n}+\beta_2(\hat{h}_n,\hat{d}_n)\frac{\alpha_2\hat{h}_n}{\hat{h}_n^2+\hat{d}_n^2}=0,\\
&\frac{W_n\beta_2(\hat{h}_n,\hat{d}_n)}{(\hat{h}_n^2+\hat{d}_n^2)^{-\frac{\alpha_2}{2}}}-\frac{W_B\beta_2(\hat{h}_n,d-\hat{d}_n)}{(\hat{h}_n^2+(d-\hat{d}_n)^2)^{-\frac{\alpha_2}{2}}}=0.
\end{aligned}\tag{31}$$

In summary, the optimum altitude and the optimum distances for the multi-hop single link setting can be found by solving N nonlinear equations. In the special case when $\frac{P_i}{W_i}=\frac{P}{W}$, it can be shown that one only needs to solve two nonlinear equations. For the dual-hop multi-link setting, one needs to solve two nonlinear equations and in the special case, one nonlinear equation for the optimum altitude and the optimum distance is always $\frac{d}{2}$. In practice, the optimum altitude takes the maximum of h_{min} and the solution from the equation.

C. Type C Channel Model

In this type, the path loss model parameters of the air-to-ground channel depend on the altitude only. We use $\alpha_2(h)$ and $\beta_2(h)$ to replace α_2 and β_2, respectively, to show this dependence explicitly. They are defined in (7).

For the multi-hop AF, the optimum altitude satisfies

$$\begin{aligned}
&\frac{W_1[\frac{\partial\beta_2(\hat{h})}{\partial\hat{h}}+\beta_2(\hat{h})(\frac{\partial\alpha_2(\hat{h})}{2\partial\hat{h}}\ln(\hat{h}^2+\hat{d}_1^2)+\frac{\alpha_2(\hat{h})\hat{h}}{\hat{h}^2+\hat{d}_1^2})]}{P_1\Omega(\hat{h}^2+\hat{d}_1^2)^{\frac{-\alpha_2(\hat{h})}{2}}[1+\frac{W_1}{P_1\Omega}\beta_2(\hat{h})(\hat{h}^2+\hat{d}_1^2)^{\frac{\alpha_2(\hat{h})}{2}}]}\\
&+\frac{W_N[\frac{\partial\beta_2(\hat{h})}{\partial\hat{h}}+\beta_2(\hat{h})(\frac{\partial\alpha_2(\hat{h})}{2\partial\hat{h}}\ln(\hat{h}^2+(d-\hat{d}_{N-1})^2)+\frac{\alpha_2(\hat{h})\hat{h}}{\hat{h}^2+(d-\hat{d}_{N-1})^2})]}{P_N\Omega(\hat{h}^2+(d-\hat{d}_{N-1})^2)^{-\frac{\alpha_2(\hat{h})}{2}}[1+\frac{W_N}{P_N\Omega}\beta_2(\hat{h})(\hat{h}^2+(d-\hat{d}_1)^2)^{\frac{\alpha_2(\hat{h})}{2}}]}=0,
\end{aligned}\tag{32}$$

and the optimum distances satisfy

$$\frac{\frac{W_1\beta_2(\hat{h})}{P_1\Omega}(\hat{h}^2+\hat{d}_1^2)^{\frac{\alpha_2(\hat{h})}{2}-1}\alpha_2(\hat{h})\hat{d}_1}{1+\frac{W_1\beta_2(\hat{h})}{P_1\Omega}(\hat{h}^2+\hat{d}_1^2)^{\frac{\alpha_2(\hat{h})}{2}}}=\frac{\frac{W_2\beta_1}{P_2\Omega}(\hat{d}_2-\hat{d}_1)^{\alpha_1-1}\alpha_1}{1+\frac{W_2\beta_1}{P_2\Omega}(\hat{d}_2-\hat{d}_1)^{\alpha_1}}=\cdots$$
$$=\frac{\frac{W_N\beta_2(\hat{h})}{P_N\Omega}(\hat{h}^2+(d-\hat{d}_{N-1})^2)^{\frac{\alpha_2(\hat{h})}{2}-1}\alpha_2(\hat{h})(d-\hat{d}_{N-1})}{1+\frac{W_N\beta_2(\hat{h})}{P_N\Omega}(\hat{h}^2+(d-\hat{d}_{N-1})^2)^{\frac{\alpha_2(\hat{h})}{2}}}, \tag{33}$$

where

$$\frac{\partial\beta_2(h)}{\partial h}=2.05\times10^{-0.85}h^{1.05},$$
$$\frac{\partial\alpha_2(h)}{\partial h}=-\frac{0.9}{h\ln 10}. \tag{34}$$

For multi-hop DF γ_{ee2}, the optimum altitude and distances satisfy

$$\frac{\partial\beta_2(\hat{h})}{\partial\hat{h}}+\beta_2(\hat{h})(\frac{\partial\alpha_2(\hat{h})}{2\partial\hat{h}}\ln(\hat{h}^2+\hat{d}_1^2)+\frac{\alpha_2(\hat{h})\hat{h}}{\hat{h}^2+\hat{d}_1^2})=0, \tag{35}$$

$$\frac{W_1\beta_2(\hat{h})}{P_1\Omega}(\hat{h}^2+\hat{d}_1^2)^{\frac{\alpha_2(\hat{h})}{2}}=\frac{W_2\beta_1}{P_2\Omega}(\hat{d}_2-\hat{d}_1)^{\alpha_1}=\cdots=\frac{W_N\beta_2(\hat{h})}{P_N\Omega}(\hat{h}^2+(d-\hat{d}_{N-1})^2)^{\frac{\alpha_2(\hat{h})}{2}}. \tag{36}$$

Next, we discuss the dual-hop multi-link setting. In this case, for χ_{ee1}, one has

$$\frac{W_n[\frac{\partial\beta_2(\hat{h}_n)}{\partial\hat{h}_n}+\beta_2(\hat{h}_n)(\frac{\partial\alpha_2(\hat{h}_n)}{2\partial\hat{h}_n}\ln(\hat{h}_n^2+\hat{d}_n^2)+\frac{\alpha_2(\hat{h}_n)\hat{h}_n}{\hat{h}_n^2+\hat{d}_n^2})]}{P_A\Omega(\hat{h}_n^2+\hat{d}_n^2)^{\frac{-\alpha_2(\hat{h}_n)}{2}}[1+\frac{W_n}{P_A\Omega}\beta_2(\hat{h}_n)(\hat{h}_n^2+\hat{d}_n^2)^{\frac{\alpha_2(\hat{h}_n)}{2}}]}$$
$$+\frac{W_B[\frac{\partial\beta_2(\hat{h}_n)}{\partial\hat{h}_n}+\beta_2(\hat{h}_n)(\frac{\partial\alpha_2(\hat{h}_n)}{2\partial\hat{h}_n}\ln(\hat{h}_n^2+(d-\hat{d}_n)^2)+\frac{\alpha_2(\hat{h}_n)\hat{h}_n}{\hat{h}_n^2+(d-\hat{d}_n)^2})]}{P_n\Omega(\hat{h}_n^2+(d-\hat{d}_n)^2)^{-\frac{\alpha_2(\hat{h}_n)}{2}}[1+\frac{W_B}{P_n\Omega}\beta_2(\hat{h}_n)(\hat{h}_n^2+(d-\hat{d}_n)^2)^{\frac{\alpha_2(\hat{h}_n)}{2}}]}=0, \tag{37}$$

$$\frac{\frac{W_n\beta_2(\hat{h}_n)}{P_A\Omega}(\hat{h}_n^2+\hat{d}_n^2)^{\frac{\alpha_2(\hat{h}_n)}{2}-1}\hat{d}_n}{1+\frac{W_n\beta_2(\hat{h}_n)}{P_A\Omega}(\hat{h}_n^2+\hat{d}_n^2)^{\frac{\alpha_2(\hat{h}_n)}{2}}}=\frac{\frac{W_B\beta_2(\hat{h}_n)}{P_n\Omega}(\hat{h}_n^2+(d-\hat{d}_n)^2)^{\frac{\alpha_2(\hat{h}_n)}{2}-1}(d-\hat{d}_n)}{1+\frac{W_B\beta_2(\hat{h}_n)}{P_n\Omega}(\hat{h}_n^2+(d-\hat{d}_n)^2)^{\frac{\alpha_2(\hat{h}_n)}{2}}}, \tag{38}$$

to find the optimum values of h_n and d_n. For χ_{ee2}, one has

$$\frac{\partial\beta_2(\hat{h}_n)}{\partial\hat{h}_n}+\beta_2(\hat{h}_n)(\frac{\partial\alpha_2(\hat{h}_n)}{2\partial\hat{h}_n}\ln(\hat{h}_n^2+\hat{d}_n^2)+\frac{\alpha_2(\hat{h}_n)\hat{h}_n}{\hat{h}_n^2+\hat{d}_n^2})=0, \tag{39}$$

$$\frac{W_n}{P_A\Omega}(\hat{h}_n^2+\hat{d}_n^2)^{\frac{\alpha_2(\hat{h}_n)}{2}}=\frac{W_B}{P_n\Omega}(\hat{h}_n^2+(d-\hat{d}_n)^2)^{\frac{\alpha_2(\hat{h}_n)}{2}}. \tag{40}$$

In the above derivation, the results for the multi-hop AF and DF in three different UAV channels have never been obtained in the literature before. The results for the dual-hop AF and DF in Type B and Type C channels have not been obtained before either, due to the

special characteristics of Type B and Type C channels. The only result that is similar to those in the literature [23] - [27] is the derivation for the dual-hop AF and DF in Type A channel. Nevertheless, it is presented here for completeness and for comparison. Thus, most of our results are new.

IV. Performance Comparison

In this section, we compare the two relaying options using multiple UAVs in terms of the outage and the bit error rate (BER). In [39], using the method proposed in [40], very accurate approximations to the outage and the BER of multi-hop AF have been derived. In particular, for γ_{ee1}, one has the outage as [39]

$$P_O(\gamma_{th}) = \frac{1}{2} + \int_0^{\frac{\pi}{2}} Re\{\frac{e^{-j\tan\theta/\gamma_{th}}\Phi(\tan\theta)}{j\pi\tan\theta}\}\sec^2\theta d\theta, \tag{41}$$

where $Re\{\cdot\}$ takes the real part of a complex number and $\Phi(\cdot)$ is the characteristic function given by $\Phi(\omega) = M(s)|_{s=-j\omega}$, $M(s) = \prod_{i=1}^{N}\left[\frac{2}{\Gamma(m)}\left(\frac{m\hat{c}s}{\Gamma_i}\right)^{\frac{m}{2}} K_m(2\sqrt{\frac{m\hat{c}s}{\Gamma_i}})\right]$ is the moment-generating function, $K_m(\cdot)$ is the m-th order modified Bessel function of the second type, $\hat{c} = \frac{\sum_{i=1}^{N}\frac{1}{\Gamma_i}}{\prod_{i=1}^{N}(1+\frac{1}{\Gamma_i})-1}$ is a constant, while $\Gamma_i = \frac{P_i\Omega}{W_iU(r_i)}$ for $i = 1$ *or* N and $\Gamma_i = \frac{P_i\Omega}{W_iV(r_i)}$ for $i = 2, \cdots, N-1$ is the average SNR of the i-th hop. To find them, the optimum altitude and the optimum distances derived in the previous section can be used to calculate r_i.

Also, for γ_{ee1}, the BER for binary phase shift keying is [39]

$$\bar{P}_e = \frac{1}{2} - \frac{1}{\pi}\int_0^{\frac{\pi}{2}} \frac{M(\tan\theta)\sin(2\sqrt{\tan\theta})}{\tan\theta}\sec^2\theta d\theta. \tag{42}$$

For the multi-hop DF γ_{ee2}, the outage and the BER can be calculated as [30]

$$P_O(\gamma_{th}) = 1 - \prod_{i=1}^{N}(1 - \frac{\gamma(m, m\gamma_{th}/\Gamma_i)}{\Gamma(m)}), \tag{43}$$

and

$$\bar{P}_e = \int_0^{\infty}\frac{e^{-x}}{\sqrt{x}}[1 - \prod_{i=1}^{N}(1 - \frac{\gamma(m, mx/\Gamma_i)}{\Gamma(m)})]dx, \tag{44}$$

respectively, where $\Gamma(\cdot)$ is the Gamma function and $\gamma(\cdot,\cdot)$ is the incomplete Gamma function. The outage probability of multi-hop DF is defined as $P_O(\gamma_{th}) = Pr\{\gamma_{ee2} < \gamma_{th}\}$ in this paper. Using (10), this gives $Pr\{\gamma_{ee2} < \gamma_{th}\} = Pr\{\min\{\gamma_1, \gamma_2, \cdots, \gamma_N\} < \gamma_{th}\} = 1 - Pr\{\min\{\gamma_1, \gamma_2, \cdots, \gamma_N\} > \gamma_{th}\} = 1 - \prod_{i=1}^{N} Pr\{\gamma_i > \gamma_{th}\} = 1 - \prod_{i=1}^{N}[1 - Pr\{\gamma_i < \gamma_{th}\}]$, where we have used the independence of the link SNRs in the third equality and $Pr\{\gamma_i < \gamma_{th}\}$

can be considered as the outage probability of the i-th hop. Thus, the overall outage of DF does depend on the hop SNRs, either indirectly via the end-to-end SNR γ_{ee2} in $Pr\{\gamma_{ee2} < \gamma_{th}\}$ or directly via the hop SNRs in $Pr\{\gamma_i < \gamma_{th}\}$. These two methods are equivalent. Specifically, the overall link will have an outage event as long as any of the hops have an outage event so that the outage events in different hops are reflected in the overall outage.

For the dual-hop multi-link setting, since selection combining is used, one has the outage and the BER as

$$P_O = F^{N-1}(\gamma_{th}), \tag{45}$$

and

$$\bar{P}_e = \frac{1}{\sqrt{4\pi}} \int_0^\infty F^{N-1}(x) \frac{e^{-x}}{\sqrt{x}} dx, \tag{46}$$

where one has [41]

$$F(x) = 1 - \frac{2m^m (m-1)! e^{-\frac{m}{\Gamma_1}x - \frac{m}{\Gamma_2}x}}{\Gamma_2^m \Gamma(m)\Gamma(m)} \sum_{i_1=0}^{m_1-1} \sum_{i_2=0}^{i_1} \sum_{i_3=0}^{m-1} \frac{\binom{i_1}{i_2}\binom{m-1}{i_3}}{i_1!} (\frac{m}{\Gamma_2})^{\frac{i_2-i_3-1}{2}} (\frac{m}{\Gamma_1})^{\frac{2i_1-i_2+i_3+1}{2}}$$
$$x^{\frac{2i_1+2m-i_2-i_3-1}{2}} (x+1)^{\frac{i_2+i_3+1}{2}} K_{i_2-i_3-1}(2\sqrt{\frac{m^2 x(1+x)}{\Gamma_1\Gamma_2}}), \tag{47}$$

for AF χ_{ee1}, and

$$F(x) = 1 - (1 - \frac{\gamma(m, mx/\Gamma_1)}{\Gamma(m)})(1 - \frac{\gamma(m, mx/\Gamma_2)}{\Gamma(m)}), \tag{48}$$

for DF χ_{ee2}. In the above equations, $\Gamma_1 = \frac{P\Omega}{WU(\sqrt{h_n^2+d_n^2})}$ and $\Gamma_2 = \frac{P\Omega}{WU(\sqrt{h_n^2+(d-d_n)^2})}$, where h_n and d_n can be replaced by the optimum altitude and distance calculated in the previous section. These outage and BER expressions have been extensively studied and verified by simulation in the literature. Interested readers can find more details in [39], [30] and [41] and the references therein.

V. Numerical Results and Discussion

In this section, numerical examples of the results derived in the previous sections are presented. Since the optimum altitudes and distances depend on the average fading power only, no channel fading is used to find these optimum locations but channel fading is used in the numerical results to calculate the outage and bit error rate, as can be seen from Section IV. In the calculation, we set $P = 10\ dBm$, $W = -100\ dBm$, $m = 1$ and $\Omega = 1$. Other cases and settings can be examined in a similar way but due to the limited space, we do not discuss them here.

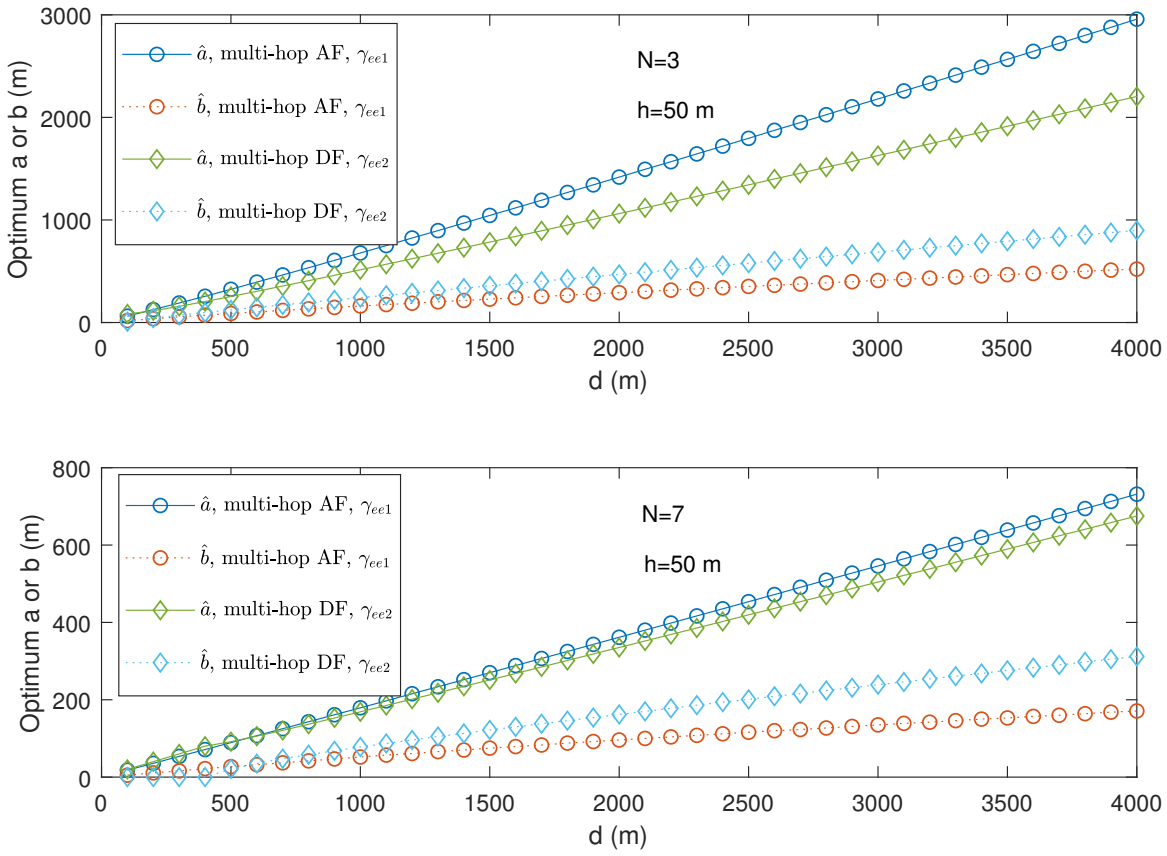

Figure 2. Optimum a and b vs. d for the multi-hop single link setting in Type A channel model.

A. *Type A Channel Model*

In this case, we set $f = 2\ GHz$ and the path loss model parameters are calculated by (5). For Type A channel model, the optimum altitudes for both multi-hop single link and dual-hop multi-link are zero or the minimum allowed safe altitude, and the optimum distance for the dual-hop multi-link setting is always $\frac{d}{2}$. Thus, they are not discussed here and we only examine the optimum distances for the multi-hop single link setting. We set a practical limit of $h_{min} = 50\ m$. Note that the optimum distances can be calculated from the optimum a and b using (17).

Fig. 2 shows the optimum a and b vs. d for the multi-hop single link setting in Type A channel model. Several observations can be made. Firstly, the optimum values of a and b increase linearly with d, when N is fixed. This agrees with intuition, as the distances between nodes will increase when they are used to cover a longer distance. Secondly, DF has a smaller $\hat{a}$ than AF and hence, a larger $\hat{b}$ than AF, under the same conditions. This means that in multi-hop DF, the

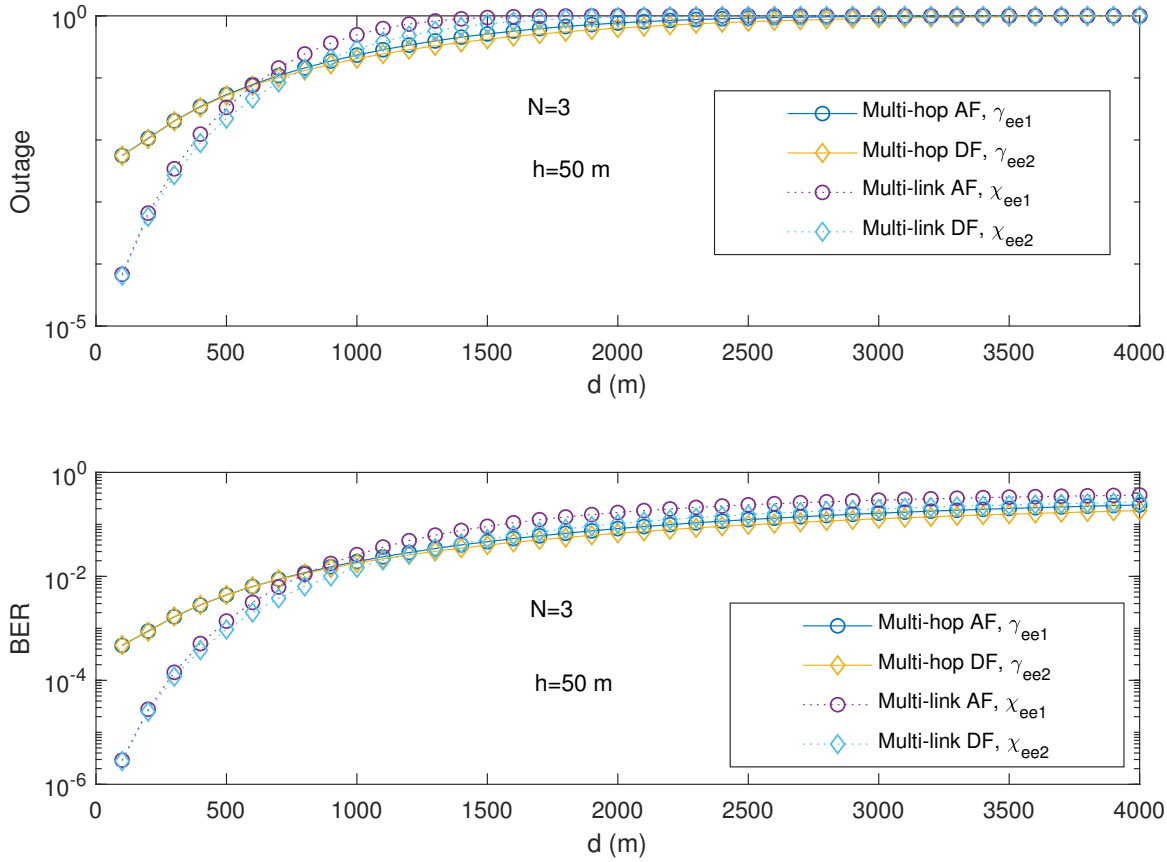

Figure 3. Outage and BER vs. d for Type A channel model when $N = 3$.

optimum UAV spacing is smaller and the distance between source (or destination) and the UAV is larger than multi-hop AF. Thus, DF may be more suitable for a large disaster-affected area that requires longer distance between the ground and the UAV. Thirdly, when N increases, the spacing between nodes decreases, as expected. The difference between AF and DF also decreases when N increases. It can also be shown that the altitude has very limited effect on the optimum values of a and b. To save space, it is not presented here.

Using the derived optimum distances, Figs. 3 and 4 compare the outage and BER performance of the multi-hop single link setting with those of the dual-hop multi-link setting. Several important observations can be made. Firstly, as the distance increases, the outage and BER performances degrade in all cases, as more path loss will be incurred in each hop for a fixed number of UAV relays. Secondly, the performance of the multi-hop single link setting is better than that of the dual-hop multi-link setting when d is large and worse when d is small. For example, in Fig. 4

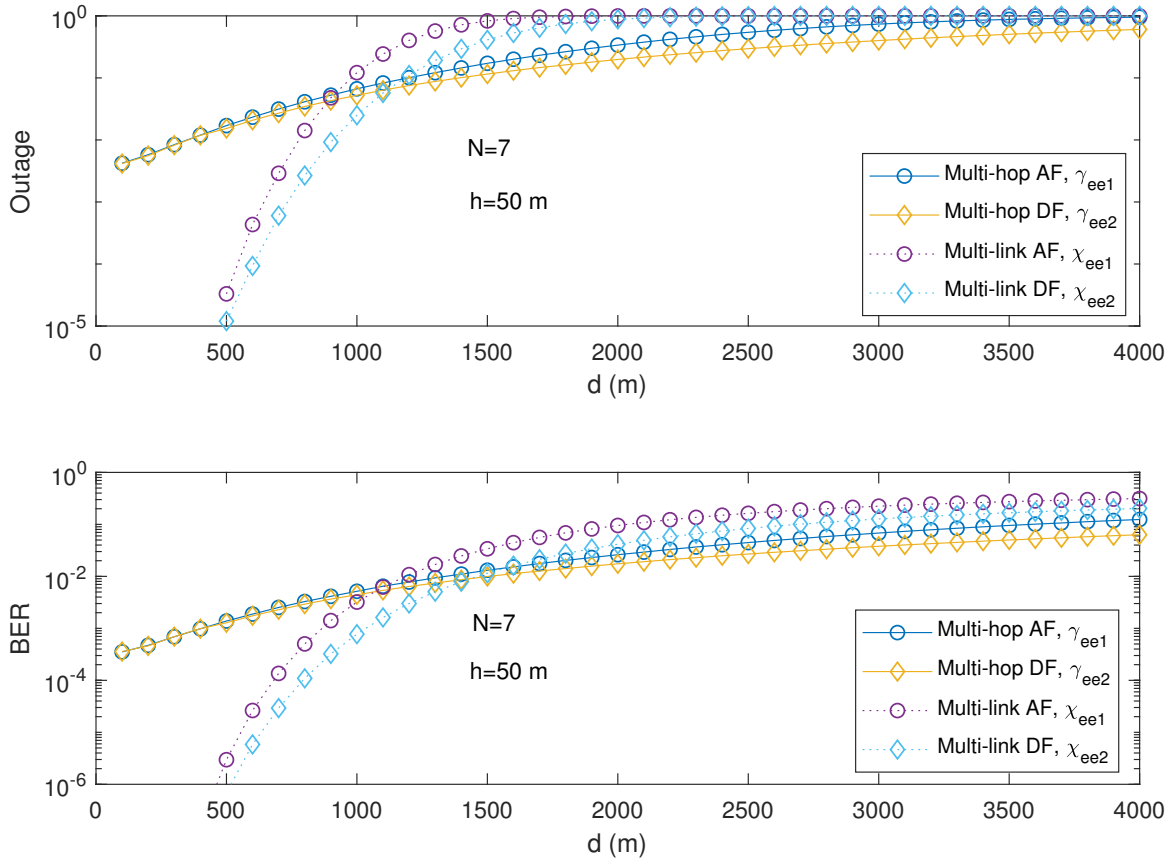

Figure 4. Outage and BER vs. d for Type A channel model when $N = 7$.

when $N = 7$, the multi-link setting has lower outage and BER than the multi-hop setting when $d < 1000\ m$. This important observation implies that, when multiple UAVs are used to cover a long distance, one should form a multi-hop single link relaying system and otherwise form a dual-hop multi-link relaying system. Our results quantify the threshold distances in different cases for best design choices. Thirdly, it is also noted that DF outperforms AF in most cases for both multi-hop and multi-link settings. Thus, DF is preferred in applications where performance is more important than complexity.

B. Type B Channel Model

In this case, we consider the suburban area where $a' = 5.0188$, $b' = 0.3511$, $\eta_{LOS} = 0.1dB$ and $\eta_{NLOS} = 21dB$ for (6). We choose $f = 2\ GHz$ and $h_{min} = 1\ m$. For the special case when all the transmission SNRs are the same for all hops, the optimum distances for the dual-hop

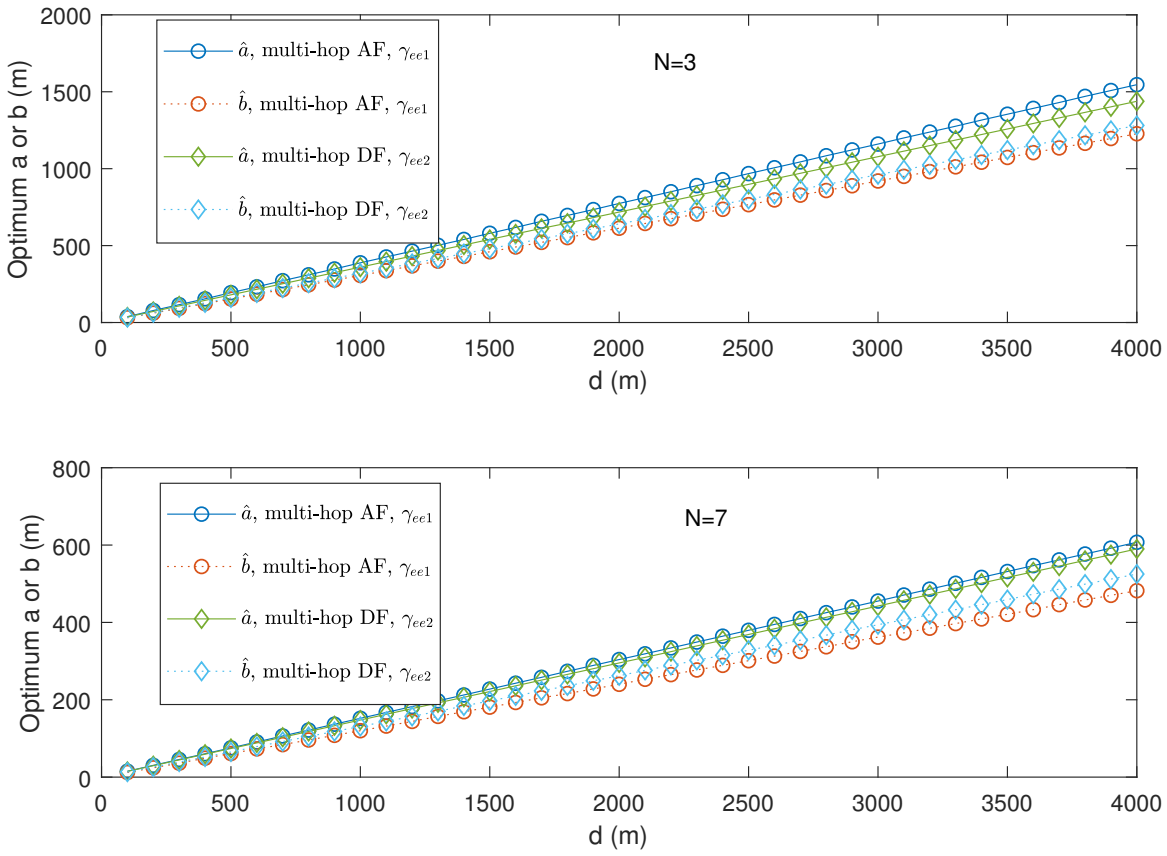

Figure 5. Optimum a and b vs. d in the multi-hop single link setting for Type B channel model.

multi-link setting are always $\frac{d}{2}$. Thus, we only examine the optimum distances for the multi-hop single link setting and the optimum altitudes for both settings.

Fig. 5 shows the optimum a and b in the multi-hop single link setting. Again, the optimum a and b increase linearly with d in the cases considered. The UAV spacing decreases when N increases, and DF has a smaller optimum a and larger optimum b than AF. Fig. 6 shows the optimum h in both settings, for Type B channel model. Since the optimum altitudes for χ_{ee1}, and χ_{ee2} are the same for the multi-link setting, there is only one curve for the multi-link case. One can see that the optimum altitude in all cases increases linearly with the distance d. However, the multi-link case has a larger optimum altitude than the multi-hop case, as high altitude is required for the dual-hop multi-link setting in order to reduce path loss. The optimum altitude for the multi-link case does not depend on N, as these UAVs operate independently for each link. The optimum altitude for the multi-hop single link case decreases with N, as larger N

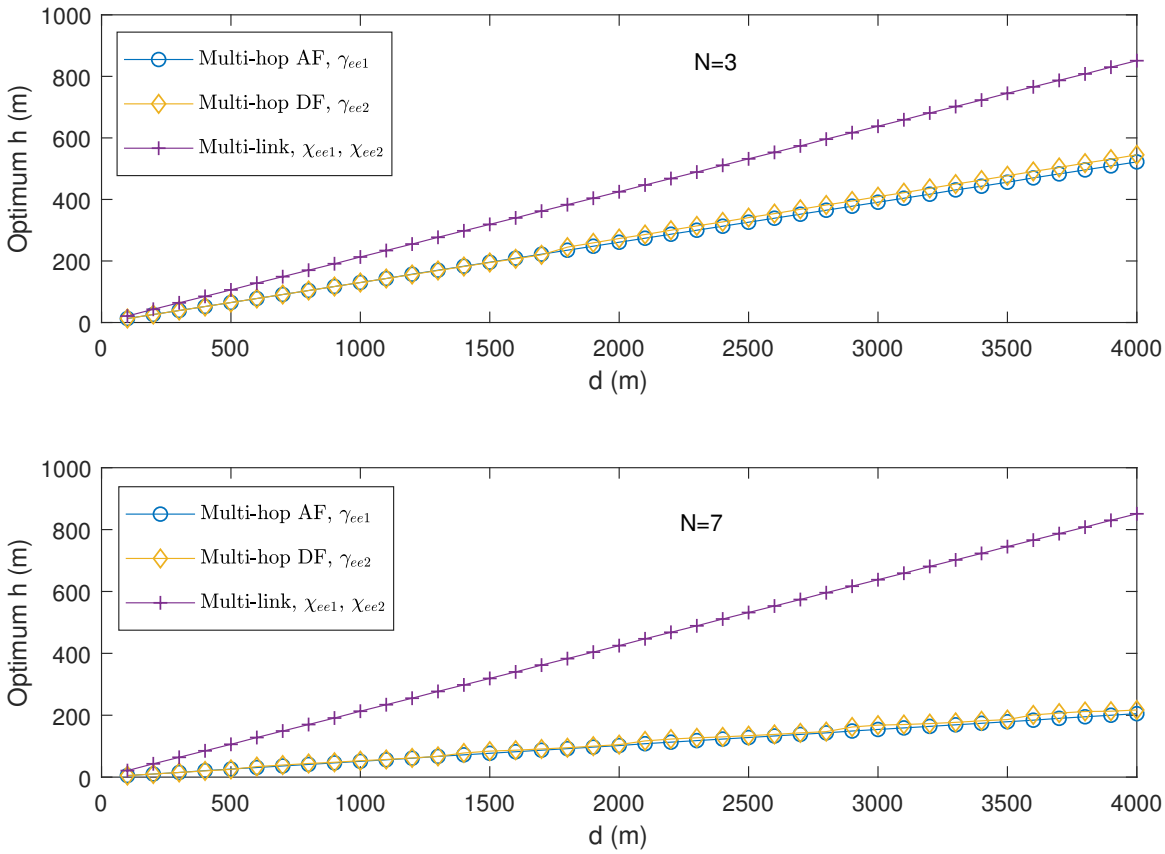

Figure 6. Optimum h vs. d for Type B channel model.

means less spacing between UAVs and hence, lower altitude to keep the elevation angle.

Fig. 7 compares the multi-hop single link setting with the dual-hop multi-link setting. In this case, there is no crossover between the multi-hop single link setting and the dual-hop multi-link setting, but their performances are indistinguishable at large distances. In all cases, the dual-hop multi-link setting outperforms the multi-hop single link setting. Thus, for Type B channel model, it is beneficial to use multiple UAVs to form a dual-hop multi-link relaying system. This is because the diversity gain achieved by the multiple links always outweighs the smaller path loss achieved by multiple hops, or the path loss in the air-to-ground channel is not large enough. One can also see that DF is better than AF in this figure. Similar observations can be made for $N = 7$ and to save space, it is not presented here.

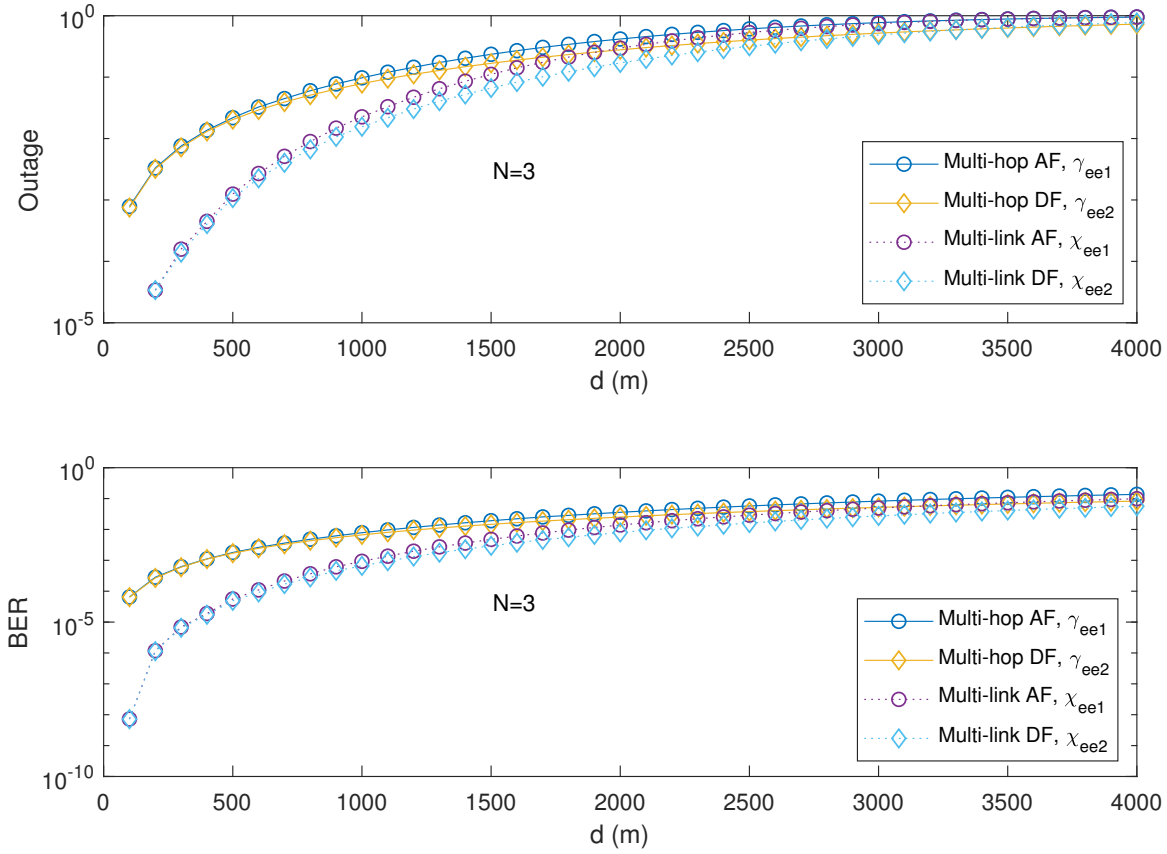

Figure 7. Outage and BER vs. d for Type B channel model when $N = 3$.

C. Type C Channel Model

In this model, we set $f = 800\ MHz$ to be consistent with the measurement in [28]. Also, the altitude is restricted as $1 \leq h \leq 120\ m$ imposed by [28] so that $h_{min} = 1\ m$. Since the opitmum distance is always $\frac{d}{2}$ for the dual-hop multi-link setting, we only examine the optimum distances for the multi-hop single link setting and the optimum altitudes for both settings.

Fig. 8 shows the optimum a and b that can be used to calculate the optimum distances in the multi-hop single link setting. In this figure, DF again has a smaller optimum a and a larger optimum b than AF in most cases. Interestingly, unlike the other channel models, in Type C channel model, $\hat{a}$ crosses with $\hat{b}$, suggesting that for large distances of d, there should be less spacing between source (or destination) and UAV than between UAVs. The threshold increases with N. Fig. 9 shows the optimum altitude for both settings in Type C channel model. There is only one curve for the multi-link case, because χ_{ee1} and χ_{ee2} have the same optimum altitude.

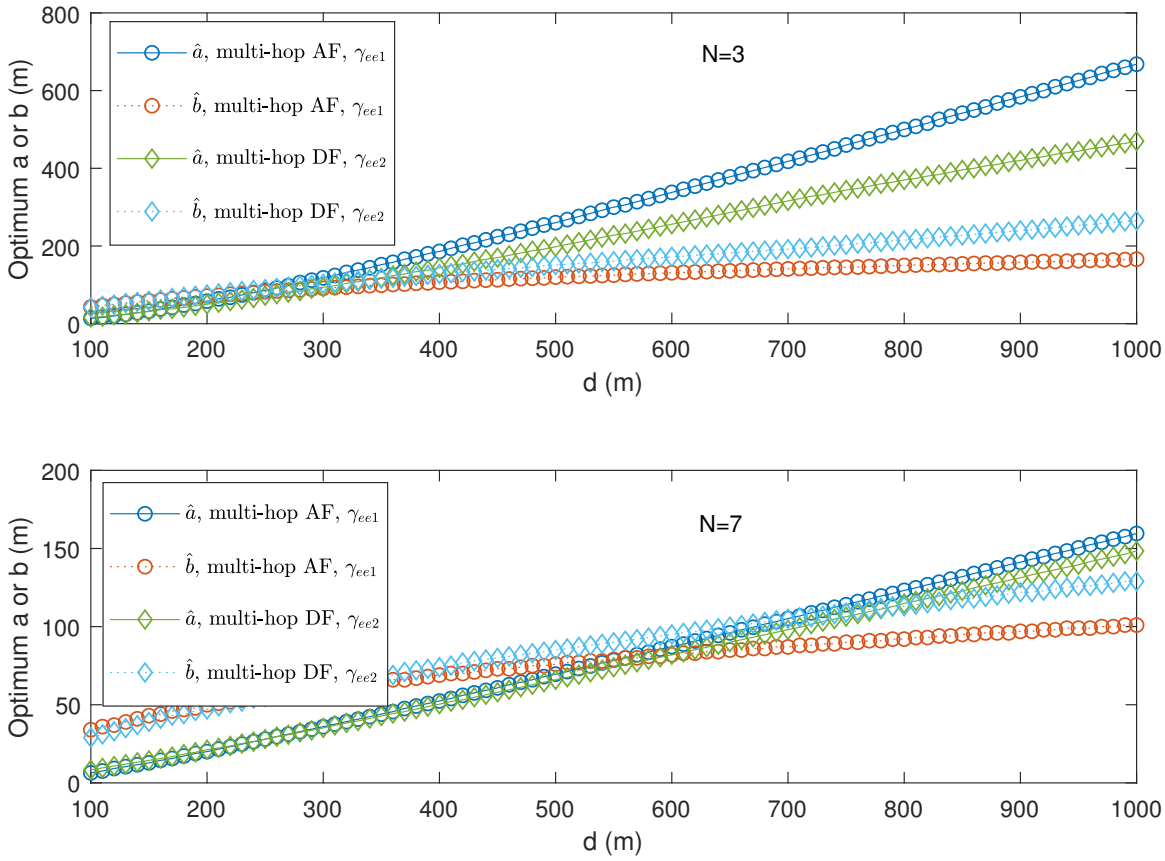

Figure 8. Optimum a and b vs. d in the multi-hop single link setting for Type C channel model.

One can see that for multi-hop AF, the optimum altitude is always 1 meter in this figure, as in these cases, the increase of path loss in β_2 cannot be compensated by the decrease of the path loss exponent α_2, when h increases. For multi-hop DF, the observation is very similar, except that when $N = 3$, the optimum altitude starts to increase with d when $d > 700\ m$. On the other hand, for the dual-hop multi-link setting, the optimum altitude starts from 1 meter and increases with d when $d > 400\ m$ and then stay at 120 meters when $d > 650\ m$, suggesting that low altitude should be used for small distance and high altitude should be used for large distance. This is mainly caused by the limitation of the model in [28] that the altitude must be between 1 meter and 120 meters. Fig. 10 compares the multi-hop single link setting with the dual-hop multi-link setting. In this case, the dual-hop multi-link setting always has smaller outage and BER than the multi-hop single link setting, and the performance difference is considerable. Hence, the multiple UAVs should be used to form multiple links in this channel model.

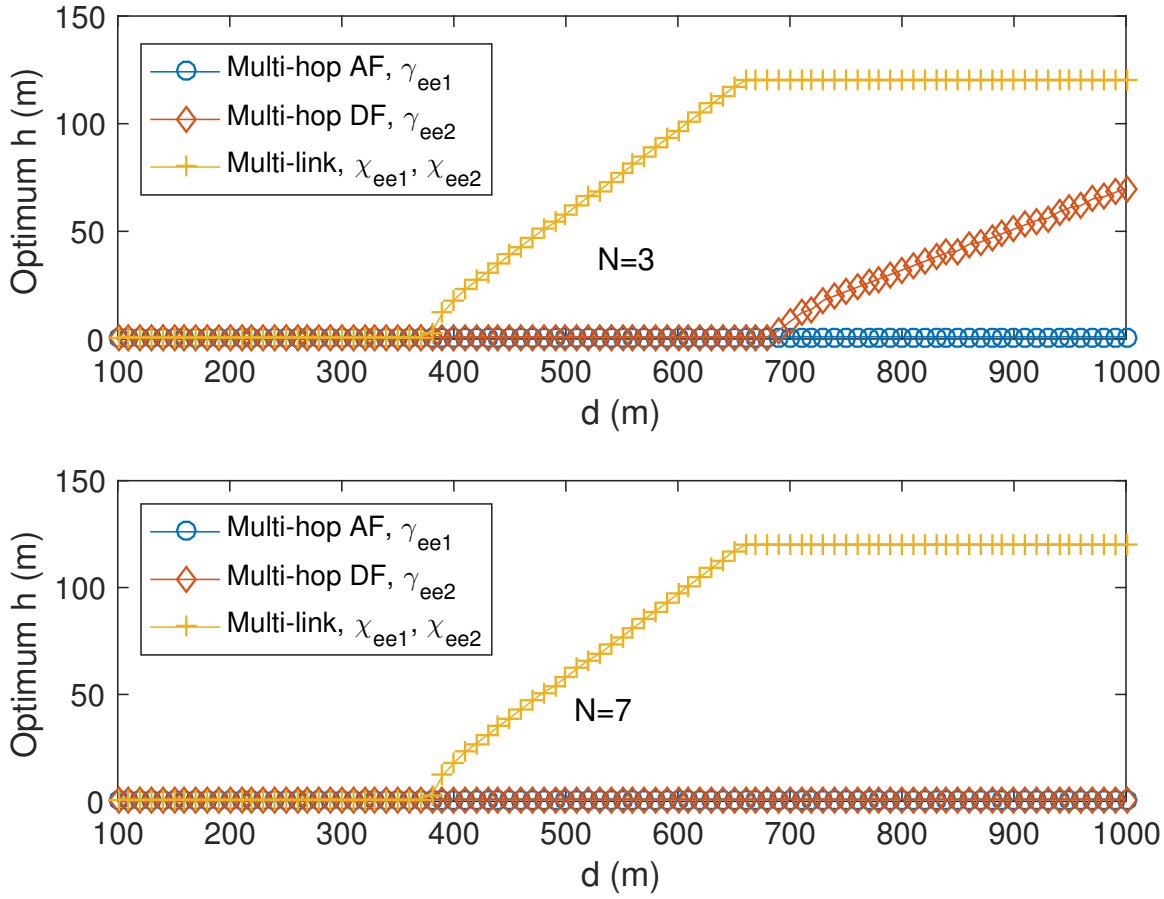

Figure 9. Optimum h vs. d for Type C channel model.

Note that, in the most general case when all UAVs have different transmission SNRs, up to N non-linear equations need to be solved in order to find the optimum altitudes and distances. The computational complexity also increases when N increases for larger systems. In our calculation, we solved four non-linear equations in Type B channel model for 7 UAVs by using MATLAB that runs on a desktop with i7-3770 CPU and 16 G memory. This takes about 2.4 seconds, which seems to be reasonable. Also, N cannot be too large, as this not only increases the computational complexity but also increases the control overhead too. It is very difficult to implement coordination and collision avoidance for a large swarm. Thus, practical systems may not have a large N. Moreover, the computation is on-off and can be performed offline, as the parameters of d, Ω, P and W are normally fixed. Thus, even for large systems, as long as the computation is performed well in advance, this may not be an issue. Finally, if the UAVs use the same transmission SNR to save control overheads, only one or two non-linear equations

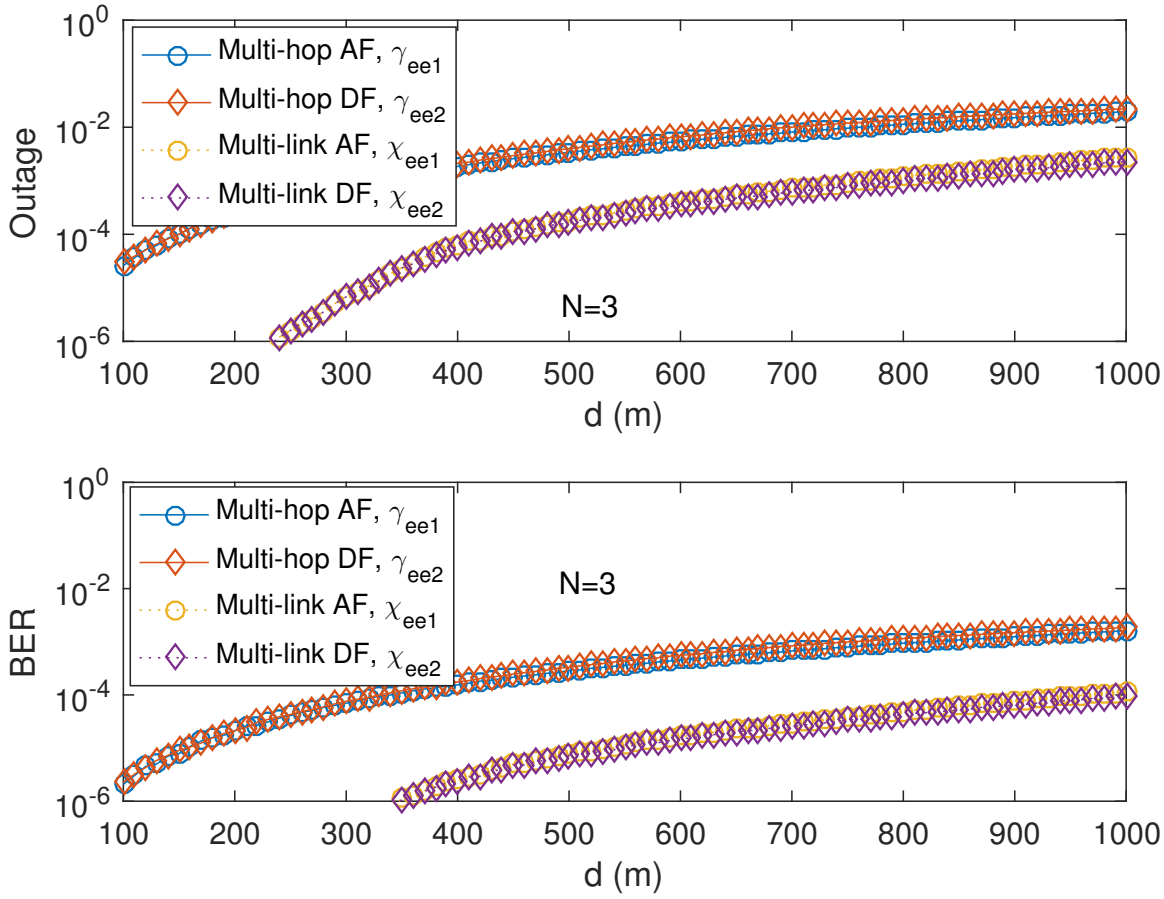

Figure 10. Outage and BER vs. d for Type C channel model when $N = 3$.

need to be solved so that the complexity does not scale up with N. Note also that the results are presented here in terms of outage and bit error rate, while the optimization is performed for the SNR. It is very difficult to optimize the outage and the bit error rate with respect to the placement directly, due to the non-linear relationship between the SNR and the outage or bit error rate. In fact, as can be seen from Section IV, the outage and bit error rate do not have any closed-form expressions for optimization in most cases. Thus, we maximize the SNR instead, as a higher SNR generally leads to better outage and bit error rate performances.

VI. Conclusion

In this paper, the use of multiple UAVs in wireless relaying has been studied. The optimum positions of the UAVs in two typical relaying options of a single multi-hop link and multiple dual-hop links have been derived by maximizing the approximate average end-to-end SNR for both

AF and DF. The outage and the BER performances of these two options have been compared. Numerical results have shown that the multiple dual-hop links option is preferred in air-to-ground channels whose path loss parameters are functions of UAV positions. When the path loss parameters are independent of UAV positions, the multi-hop single link is a better option only for large distances between source and destination. In the comparison, it has also been shown that DF is a better option than AF. These optimizations require solutions to complicated non-linear equations. However, this only needs to be done once and can be performed offline by the ground controller before the launch of the UAV, as the optimum positions depend on constants in the propagation environment that do not change with time.

REFERENCES

[1] S. Hayat, E. Yanmaz, and R. Muzaffar, "Survey on unmanned aerial vehicle networks for civil applications: a communications viewpoint," *IEEE Commun. Surveys and Tutorials*, vol. 18, pp. 2624-2661, 4th Quarter 2016.

[2] Y. Zeng, R. Zhang, and T.J. Lim, "Wireless communications with unmanned aerial vehicles: opportunities and challenges," *IEEE Comm. Mag.*, vol. 54, pp. 36 - 42, May 2016.

[3] A. Jaziri, R. Nasri, and T. Chahed, "Congestion mitigation in 5G networks using drone relays," *Proc. IEEE WCNC 2016*, pp. 233 - 238, 2016.

[4] A. Osseiran, F. Boccardi, V. Braun , "Scenarios for 5G mobile and wireless communications: the vision of the METIS project," *IEEE Commun. Mag.*, vol. 52, pp. 26 - 35, May 2014.

[5] R. Lee, J. A. Manner, J. Kim, P. Amodio, and K. Anderson, "White Paper: The Role of deployable aerial communications architecture in emergency communications and recommended next steps," FCC Public Safety and Homeland Security Bureau, Sept. 2011.

[6] D. Orfanus, E.P. de Freitas, F. Eliassen, "Self-organization as a supporting paradigm for military UAV relay networks," *IEEE Commun. Lett.*, vol. 20, pp. 804 - 807, 2016.

[7] Y. Chen, W. Feng, G. Zheng, "Optimum placement of UAV as relays," accepted by *IEEE Communications Letters.*

[8] M. Mozaffari, W. Saad, M. Bennis, M. Debbah, "Unmanned aerial vehicle with underlaid device-to-device communications: performance and tradeoffs," *IEEE Trans. Wireless Commun.*, vol. 15, pp. 3949 - 3963, June 2016.

[9] M. Mozaffari, W. Saad, M. Bennis, M. Debbah, "Optimal transport theory for cell association in UAV-enabled cellular networks," *IEEE Commun. Lett.*, vol. 21, pp. 2053 - 2056, Sept. 2017.

[10] N. Zhao, F.R. Yu, Y. Chen, G. Gui, "Caching UAV assisted secure transmission in hyper-dense networks based on interference alignment," accepted by *IEEE Trans. Communications.*

[11] F. Cheng, S. Zhang, Z. Li, Y. Chen, N. Zhao, R. Yu, V.C.M. Leung, "UAV trajectory optimization for data offloading at the edge of multiple cells," accepted by *IEEE Transactions on Vehicular Technology.*

[12] Y. Zeng, R. Zhang, and T.J. Lim, "Throughput maximization for UAV-enabled mobile relaying systems," *IEEE Trans. Commun.*, vol. 64, pp. 4983 - 4996, Dec. 2016.

[13] Q. Wang, Z. Chen, W. Mei, and J. Fang, "Improving physical layer security using UAV-enabled mobile relaying," *IEEE Wireless Commun. Lett.*, vol. 6, pp. 310 - 313, June 2017.

[14] F. Ono, H. Ochiai, and R. Miura, "A wireless relay network based on unmanned aircraft system with rate optimization," *IEEE Trans. Wireless Commun.*, vol. 15, pp. 7699 - 7708, Nov. 2016.

[15] I.Y. Abualhaol, M.M. Matalgah, "Performance analysis of multi-carrier relay-based UAV network over fading channels," *Proc. IEEE Globecom 2010 Workshop on Wireless Networking for Unmanned Aerial Vehicles*, pp. 1811 - 1815, 2010.

[16] P. Zhan, K. Yu, A.L. Swindlehurst, "Wireless relay communications using an unmanned aerial vehicle," *IEEE SPAWC 2006*, pp. 1 - 5, 2006.

[17] E. Larsen, L. Landmark, and Ø. Kure, "Optimal UAV relay positions in multi-rate networks," *IEEE Wireless Days*, pp. 8 - 14, 2017.

[18] I. Rubin and R. Zhang, "Placement of UAVs as communication relays aiding mobile ad hoc wireless networks," *Proc. IEEE Military Communications Conference 2007*, pp. 1 - 7, 2007.

[19] P. Ladosz, H. Oh, and W.-H. Chen, "Optimal positioning of communication relay unmanned aerial vehicles in urban environments," *Proc. 2016 International Conference on Unmanned Aircraft Systems (ICUAS)*, Arlington, USA, June 2016.

[20] M. Horiuchi, H. Nishiyama, N. Kato, F. Ono, and R. Miura, "Throughput maximization for long-distance real-time data transmission over multiple UAVs," *2016 IEEE International Conference on Communications*, pp. 1 - 6, 2016.

[21] P. Vincent, I. Rubin, "A framework and analysis for cooperative search using UAV swarms," *ACM Symposium on Applied Computing*. pp. 79 - 86, 2004.

[22] H. Shakhatreh, A. Khreishah, J. Chakareski, "On the continuous coverage problem for a swarm of UAVs," *2016 IEEE Sarnoff Symposium*, 2017.

[23] J. Cannons, L.B. Milstein, K. Zeger, "An algorithm for wireless relay placement," *IEEE Trans. Wireless Commun.*, vol. 8, pp. 5564 - 5574, Nov. 2009.

[24] A. Ribeiro, X. Cai, G. Giannakis, "Symbol error probabilities for general cooperative links," *IEEE Trans. Wireless Commun.*, vol. 4, pp. 1264 - 1273, May 2005.

[25] A. Nasri, R. Schober, I.F. Blake, "Performance and optimization of amplify-and-forward cooperative diversity systems in generic noise and interference," *IEEE Trans. Wireless Commun.*, vol. 10, pp. 1132 - 1143, Apr. 2011.

[26] B. Zhu, J. Cheng, M.-S. Alouini, L. Wu, "Relay placement for FSO multihop DF systems with link obstacles and infeasible regions," *IEEE Trans. Wireless Commun.*, vol. 14, pp. 5240 - 5250, Sept. 2015.

[27] M. Bagaa, A. Chelli, D. Djenouri, T. Taleb, I. Balasingham, K. Kansanen, "Optimal placement of relay nodes over limited positions in wireless sensor networks," *IEEE Trans. Wireless Commun.*, vol. 16, pp. 2205 - 2219, Apr. 2017.

[28] N. Goddemeier and C. Wietfeld, "Investigation of air-to-air channel characteristics and a UAV specific extension to the Rice model," *2015 IEEE Globecom*, pp. 1 - 5, 2015.

[29] Y. Jing and H. Jafarkhani, "Single and multiple relay selection schemes and their achievable diversity orders," *IEEE Trans. Wireless Commun.*, vol. 8, pp. 1414 - 1423, Mar. 2009.

[30] M.O. Hasna and M.-S. Alouini, "Outage probability of multihop transmission over Nakagami fading channels," *IEEE Commun. Lett.*, vol. 7, pp. 216 - 218, May 2003.

[31] N. Ahmed, S.S. Kanhere, and S. Jha, "On the importance of link characterization for aerial wireless sensor networks," *IEEE Commun. Mag.*, vol. 54, pp. 52 - 57, May 2016.

[32] A. Al-Hourani, S. Kandeepan, S. Lardner, "Optimal LAP altitude for maximum coverage," *IEEE Wireless Commun. Lett.*, vol. 3, pp. 569 - 572, Dec. 2014

[33] R. Amorim, H. Nguyen, P. Mogensen, I.Z. Kovács, J. Wigard, T.B. Sørensen, "Radio channel modelling for UAV communication over cellular networks," *IEEE Wireless Commun. Lett.*, vol. PP, pp. 1-1, 2017.

[34] I.S. Gradshteyn, I.M. Ryzhik, *Table of Integrals, Series, and Products*, 6th Ed. San Diego, CA: Academic Press. 2000.

[35] M.K. Simon and M.-S. Alouini, *Digital Communication Over Fading Channels*, 2nd Ed. John Wiley& Sons: London, 2000.

[36] W. Khawaja, I. Guvenc, and D. Matolak, "UWB channel sounding and modeling for UAV air-to-ground propagation channels," in *Proc. IEEE Global Commun. Conf. (GLOBECOM'16)*, Washington, USA, Dec. 2016, pp. 1-7.

[37] E. Yanmaz, R. Kuschnig, and C. Bettstetter, "Achieving air–ground communications in 802.11 networks with three-dimensional aerial mobility," in *Proc. IEEE INFOCOM*, Turin, Italy, April 2013, pp. 120-124.

[38] S. Boyd, *Convex Optimization*, Cambridge University Press: Cambridge, UK. 2004.

[39] N.C. Beaulieu, G. Farhadi, and Y. Chen, "A precise approximation for performance evaluation of amplify-and-forward multihop relaying systems," *IEEE Trans. Wireless Commun.*, vol. 10, pp. 3985 - 3989, Dec. 2011.

[40] N.C. Beaulieu, Y. Chen, "An accurate approximation to the average error probability of cooperative diversity in Nakagami-m fading," *IEEE Trans. Wireless Commun.*, vol. 9, pp. 2707 - 2711, Sept. 2010.

[41] A. Bletsas, H. Shin, and M. Z. Win, "Outage optimality of opportunistic amplify-and-forward relaying," *IEEE Commun. Lett.*, vol. 11, pp. 261–263, Mar. 2007.